AD-A051 135 MASSACHUSETTS UNIV AMHERST ASTRONOMY RESEARCH FACILITY F/G 7/4
INFRARED EMISSION SPECTROSCOPY OF LOW PRESSURE GASEOUS DISCHARG--ETC(U)
NOV 77 P HANSEN, H SAKAI, J STRONG F19628-76-C-0087
UNCLASSIFIED UMASS-ARF-77-303 AFGL-TR-77-0251 NL

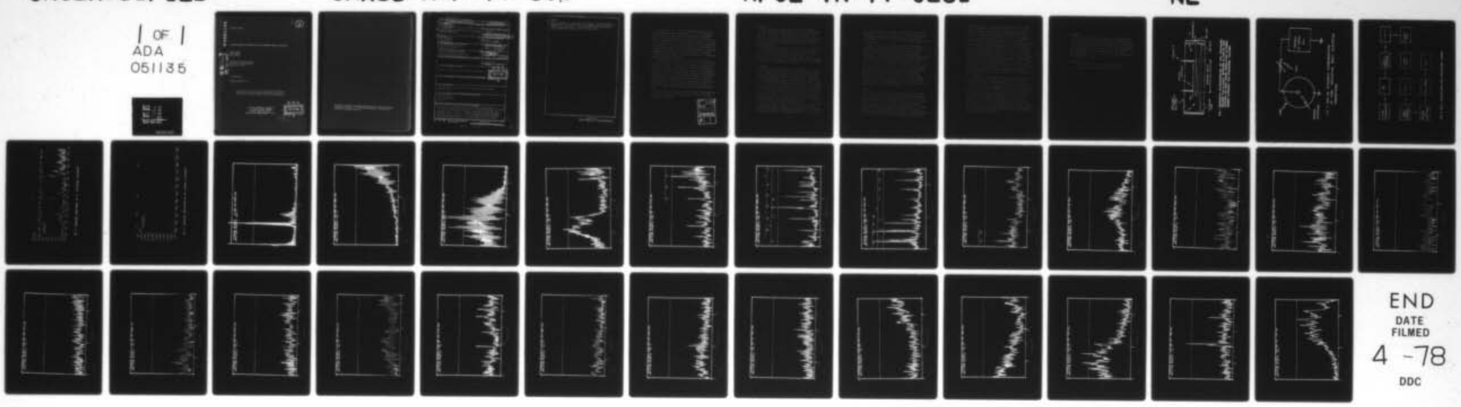

ADA051135

2

AFGL-TR-77-0251

INFRARED EMISSION SPECTROSCOPY OF LOW PRESSURE GASEOUS DISCHARGES

Peter Hansen
Hajime Sakai
John Strong

Astronomy Research Facility
University of Massachusetts
Amherst, MA 01003

1 November 1977

Scientific Report No. 1

Approved for public release; distribution unlimited.

AIR FORCE GEOPHYSICS LABORATORY
AIR FORCE SYSTEMS COMMAND
UNITED STATES AIR FORCE
HANSCOM AFB, MASSACHUSETTS 01731

Qualified requestors may obtain additional copies from the Defense Documentation Center. All others should apply to the National Technical Information Service.

UNCLASSIFIED

SECURITY CLASSIFICATION OF THIS PAGE (When Data Entered)

(19) REPORT DOCUMENTATION PAGE		READ INSTRUCTIONS BEFORE COMPLETING FORM
1. REPORT NUMBER (18) AFGL-TR-77-0251	2. GOVT ACCESSION NO.	3. RECIPIENT'S CATALOG NUMBER
4. TITLE (and Subtitle) (6) INFRARED EMISSION SPECTROSCOPY OF LOW PRESSURE GASEOUS DISCHARGES		5. TYPE OF REPORT & PERIOD COVERED Interim Scientific Report No. 1
		6. PERFORMING ORG. REPORT NUMBER (14) UMASS-ARF-77-303, SCIENTIFIC-1
7. AUTHOR(s) (10) Peter/Hansen, Hajime/Sakai, John/Strong		8. CONTRACT OR GRANT NUMBER(s) (15) F19628-76-C-0087
9. PERFORMING ORGANIZATION NAME AND ADDRESS Astronomy Research Facility University of Massachusetts Amherst, MA 01003		10. PROGRAM ELEMENT, PROJECT, TASK AREA & WORK UNIT NUMBERS 61102F 2310G401 (16) 2310 (17) G4
11. CONTROLLING OFFICE NAME AND ADDRESS Air Force Geophysics Laboratory Hanscom AFB, Massachusetts 01731 Monitor/Alastair Fairbairn/OPR		12. REPORT DATE (11) 1 November 1977
		13. NUMBER OF PAGES 37 (12) 39p.
14. MONITORING AGENCY NAME & ADDRESS(if different from Controlling Office)		15. SECURITY CLASS. (of this report) Unclassified
		15a. DECLASSIFICATION/DOWNGRADING SCHEDULE

16. DISTRIBUTION STATEMENT (of this Report)

Approved for public release; distribution unlimited.

DDC RECEIVED MAR 13 1978 B

17. DISTRIBUTION STATEMENT (of the abstract entered in Block 20, if different from Report)

18. SUPPLEMENTARY NOTES

Presented at 1977 Fall Meeting of the Optical Society of America; Toronto, Canada.

19. KEY WORDS (Continue on reverse side if necessary and identify by block number)

Emission spectra
Fourier spectroscopy
Gaseous discharge
Infrared

delta nu approx.

20. ABSTRACT (Continue on reverse side if necessary and identify by block number)

A Michelson interferometer is used to measure infrared radiation in emission from a gaseous discharge column. The discharge column is contained in a 30-meter pathlength cell using a 12-meter central electrode. By optically triple passing, the equivalent pathlength achieved through the discharge column is 36 meters. Spectral resolution near $\Delta\nu \sim 1/cm$ is obtained. Sample spectra in the 1800 - 8000/cm region are presented. The discharge column consists of a 1-meter diameter steel tube with a

next page

DD FORM 1 JAN 73 1473 EDITION OF 1 NOV 65 IS OBSOLETE
S/N 0102-014-6601

UNCLASSIFIED

SECURITY CLASSIFICATION OF THIS PAGE (When Data Entered)

406 989

Block 20

central electrode. It is powered by an AC supply. Power dissipation ranges from 1 to 4 kilowatts. Due to the discharge geometry, pressure is limited to the range of 0.1 to 0.6 torr; however, broad adjustments in current density are possible over this pressure range.

This contract is (1) to create a discharge condition similar to those existing in the upper atmosphere, and (2) to study the infrared emission spectra of atomic and molecular nature which are generated from it. The work described in this scientific report represents our effort made during the first year of a multi-year program. Our principal scheme of experiment is to utilize the technique of Fourier spectroscopy for observation of the infrared emission generated in low pressure, long pathlength flow discharge. Since an insignificant amount of information is available in literature for the laboratory study of the infrared discharge emission, our main effort has been concentrated to develop the technique most adaptable to our need.

During this phase of work, we have succeeded to produce a very stable discharge condition which is essential for the spectrometry using the Fourier technique. We believe that the problem of generating the infrared emission spectra has been solved at least to our satisfaction. The recovered spectra show a good signal-to-noise ratio with a spectral resolution of 1.0 cm^{-1}, a figure currently achieved. The interferogram recording scheme used in the measurement is antiquated and preventing us from extending the maximum path difference much beyond the presently achieved figure of 1.0 cm^{-1}. Within the next few weeks, we will introduce a new recording scheme, expecting to improve the resolution to a figure of 0.1 cm^{-1}, the limit imposed by the interferometer currently used.

The scientific report which is contained in the following pages was presented at the 1977 Fall Meeting of the Optical Society of America held at Toronto, Canada.

INTRODUCTION

This report covers work done in the first year of a multi-year contract to determine the infrared spectra of atoms and molecules under conditions similar to those existing in the upper atmosphere. Low pressure, long pathlength electronic flow discharges are generated in various gases and the resulting emission spectra are obtained by means of Fourier spectroscopy. The discharge facility and data handling system are described.

As evidence of the capability of the overall system, sample spectra are presented of some of the species (CO, CO_2, N_2, NI, OI) radiating in the 1800 to 7900 cm^{-1} spectral region. Optimum resolution to date is $\Delta\nu = .96\ cm^{-1}$. This effort continues with the current objective of increasing the resolving power of the spectra, and a substantial increase of the flow rate of the discharge to decrease the effects of contaminants.

EXPERIMENTAL

The discharge column is contained in a steel vessel (Fig. 1) one meter in diameter and 33 meters long. A 12-meter-long polished aluminum electrode is centrally suspended in the midsection of this tank. This central electrode and the tank walls form the discharge configuration.

The discharge is powered by a 10 kw variable 60 Hz supply (Fig. 2). Due to the high power dissipation, the central electrode is water cooled. Typical operating conditions are 2.5 kw ($V \cong 1000$ VAC, $I = 2.5$ A) supplied to the discharge and 1 kw dissipated in the load. The discharge may be operated in the pressure range of 200 to 600 millitorr, depending on the gas under consideration. By variation of the pressure and load, stable operating conditions can be achieved over prolonged periods of time. As the pressure range is limited, current density is essentially the only independent variable affecting discharge conditions.

The optical system consists of two 1-meter diameter, 33-meter focal length spherical mirrors. The mirrors are focused on one another, resulting in three passes through the discharge column, for an equivalent optical path of 36 meters. The resulting f/33 beam is then collimated by

a KBr lens and enters the interferometer, an Idealab IF6 that has been modified for use in the 1 to 6 micron region. The interferometer uses a CaF beamsplitter and InSb and PbS cooled detectors. Its ultimate resolving power is near $\Delta\nu \gtrsim 0.1$ cm^{-1}. The path difference is monitored with a He-Ne laser.

There are two basic data handling systems presently available or near completion. For the spectra presented in this report, the interferograms were punched on paper tape and subsequently the data was placed on a CDC 6600 computer for the Fourier transformation and subsequent plot. This method, while workable, is extremely time-consuming (slow punch rate) and has some inherent limitations as to the number of data points that may be taken (16K) and the resolution of the A/D conversion (10 BITS). This system limits resolution to about $\Delta\nu \gtrsim .6$ cm^{-1}. Near completion now is the system outlined in Fig. 3. Here the radiation from the discharge column (already chopped at 120 Hz) enters the interferometer. The detector signal (interferogram) is synchronously amplified and passed to a 12 BIT A/D convertor locked to the interferometer's laser signal. The A/D output is passed through a parallel interface to a DEC LSI 11/03 minicomputer and stored on a floppy disk. The interferogram is then transmitted via a serial interface and a time-sharing system to the CDC 6600 for processing.

RESULTS

Some earlier (1974-75) spectra of the discharge column were taken with an interferometer and data reduction system provided by Dr. Randall Murphy of AFGL. These are low resolution spectra (10 cm^{-1} < $\Delta\nu$ < 50 cm^{-1}), as the operating time of the discharge column was limited due to the fact that the central electrode at the time was not water cooled, and the overall spectrometric system was set up for low resolution. Fig. 4 shows a nitrogen flow discharge spectrum in the PbS region. The molecular electronic band structure of the $B^3\Pi_g \rightarrow A^3\Sigma_u^+$ system is indicated according to the scheme of Saum and Benesch.[1] Fig. 5 indicates the spectrum of an

oxygen flow discharge. The significant features here are atomic oxygen lines at 5549 cm^{-1}, 5485 cm^{-1}, 3773 cm^{-1}, 3617 cm^{-1}, and 3456 cm^{-1}. These have previously been identified by Saum and Benesch.[2] Both the nitrogen and oxygen spectra were compared to a black body spectrum at 2300°K. The spectral radiance values 10^{-3} to 10^{-5} W/cm^2-SR-wavenumber appear to be typical of the signal strengths that are encountered.

Fig. 6 shows the spectrum of a nitrogen flow discharge. The conditions under which this spectrum was obtained were the following: The power supplied to the discharge was $\approx$ 2 kw, i.e., 800 VAC at 2.5 amperes, and the pressure was 250 millitorr. It took 3 hours to take the spectrum; however, here the limiting factor was the speed of the paper tape punch. The flow rate was 1 ℓ/min. The discharge acts as its own chopper (120 Hz) and thus the powerline frequency is used as a reference for synchronous rectification. The spectral range covered is 1800 → 7900 cm^{-1}, the lower limit being the cutoff frequency of the InSb detector, while the upper limit is due to the sampling interval. Spectral resolution is $\Delta\nu = 1$ cm^{-1}. Figs. 7 through 30 show this spectrum in more detail in increments of 250 cm^{-1}. It should be noted that the vertical gain is not the same for all the spectra.

As perhaps could be expected, the strongest spectral features are caused by impurities CO, CO_2, and possibly OH and NH. Electronic transitions in molecular and atomic nitrogen are also observed. From 1850 cm^{-1} to 2150 cm^{-1} the CO vibration rotation bands predominate. From 2290 cm^{-1} to 2365 cm^{-1} the ν_3 fundamental band of CO_2 is clearly defined (Fig. 9). In the 2500 cm^{-1} to 3500 cm^{-1} region several band systems have been schematically indicated. The wide spacing of the emission lines in these spectra (high rotational constant $\approx$ 15 cm^{-1}) indicates vibration rotation bands of OH and NH. We feel that higher resolving power is desirable for complete analysis of this spectral region. Another CO_2 feature appears at 3700 cm^{-1}. From 3800 cm^{-1} to 6600 cm^{-1} there are some small features as yet not identified. Between 6600 and 7700 cm^{-1} we again have electronic transitions in molecular nitrogen. Also atomic nitrogen is observed at 7360 cm^{-1} and 7444 cm^{-1}.

CONCLUSION

We have shown that during the first year of this contract we have established a low pressure, long pathlength gaseous discharge facility effectively simulating conditions in the upper atmosphere. The infrared radiant flux from the discharge column is sufficient to produce spectra with good S/N. With the new data handling system, and a faster pumping system, both under construction, we will be able to produce higher resolving power ($\Delta\nu \approx .1$ cm^{-1}) emission spectra of the atmospheric gases with lower impurity content.

REFERENCES

1. K.A. Saum and W.M. Benesch, Appl. Opt. 9, 195 (1970).
2. K.A. Saum and W.M. Benesch, Appl. Opt. 9, 1419 (1970).

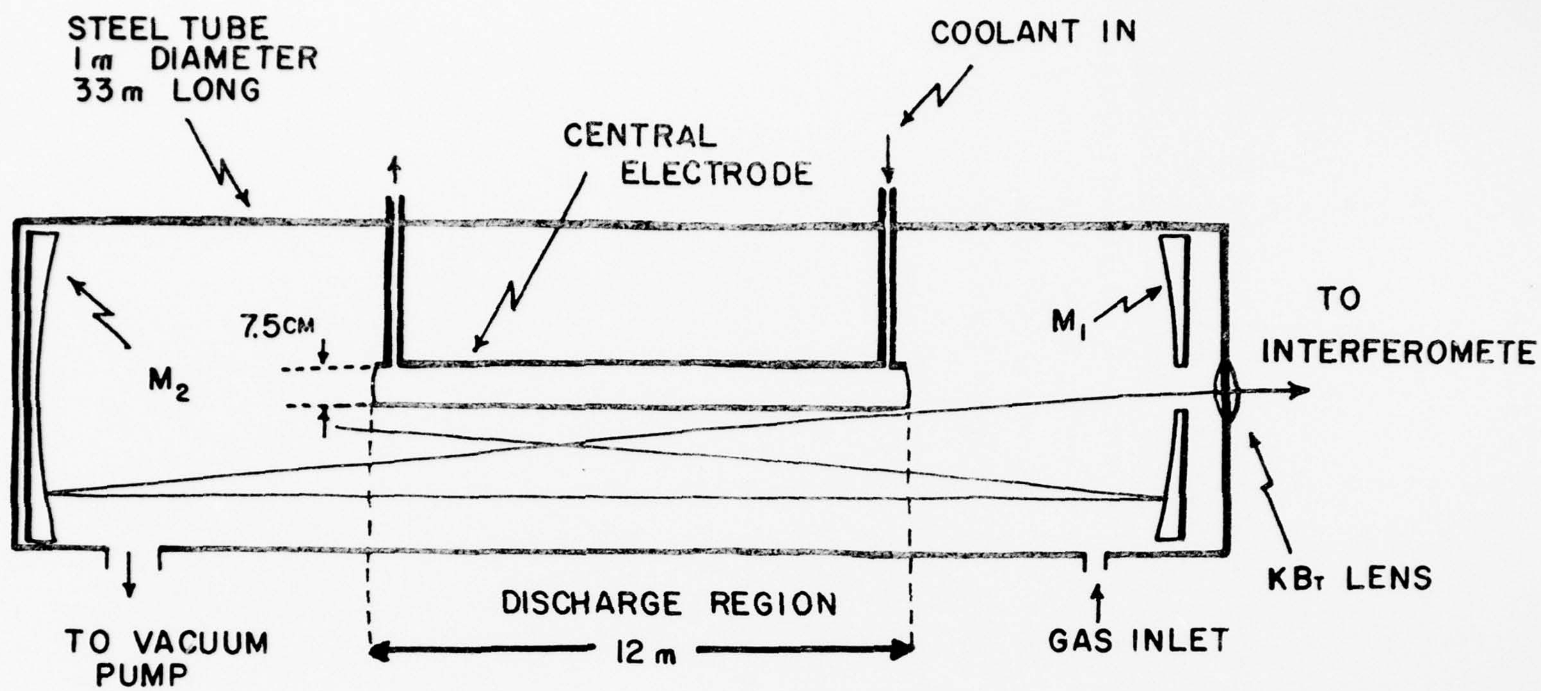

FIG. 1 SCHEMATIC REPRESENTATION OF THE DISCHARGE COLUMN (not to scale). MIRRORS M_1 AND M_2 ARE FOCUSED ON EACH OTHER RESULTING IN THREE PASSES THROUGH THE DISCHARGE COLUMN.

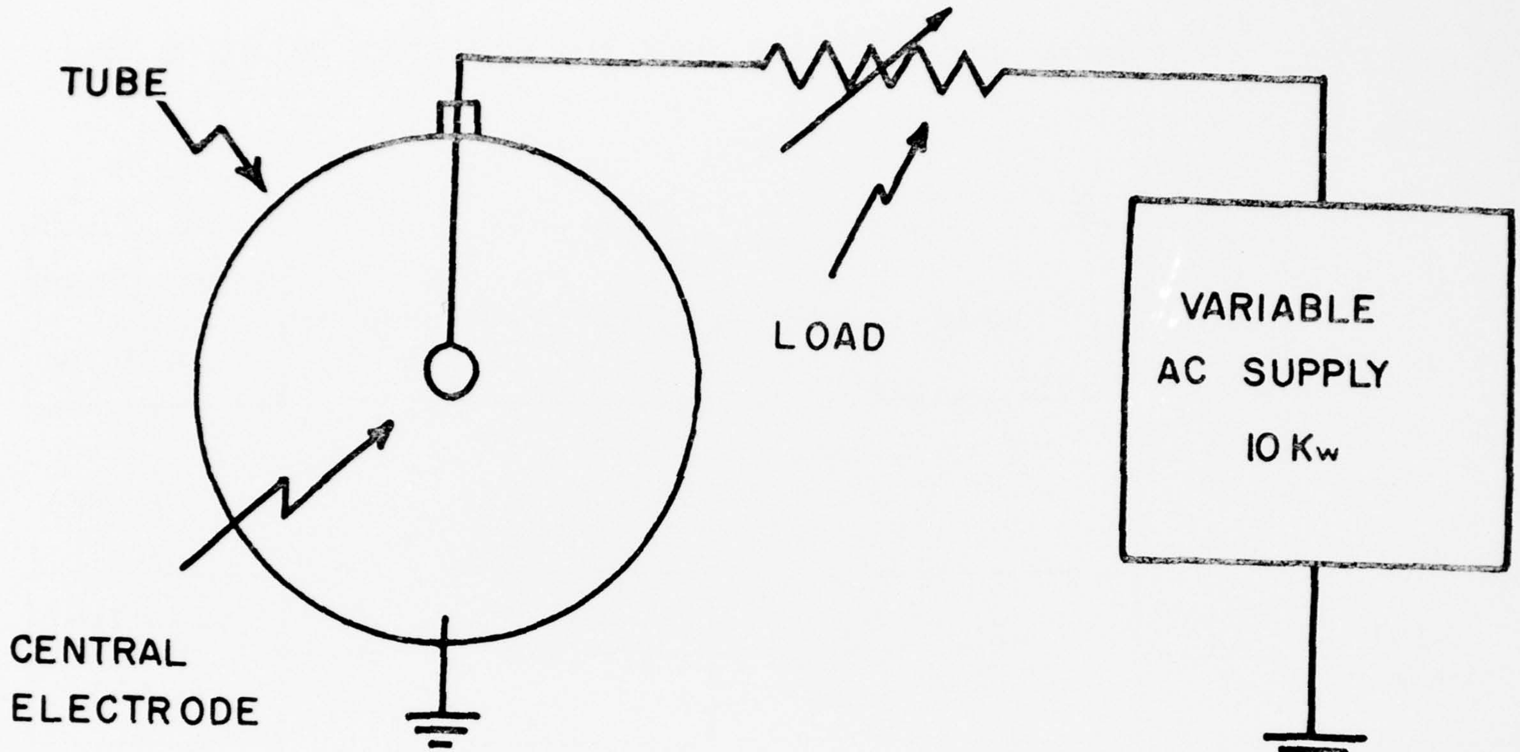

FIG. 2 END ON SCHEMATIC REPRESENTATION OF TUBE INDICATING BASIC ELECTRICAL CONNECTIONS.

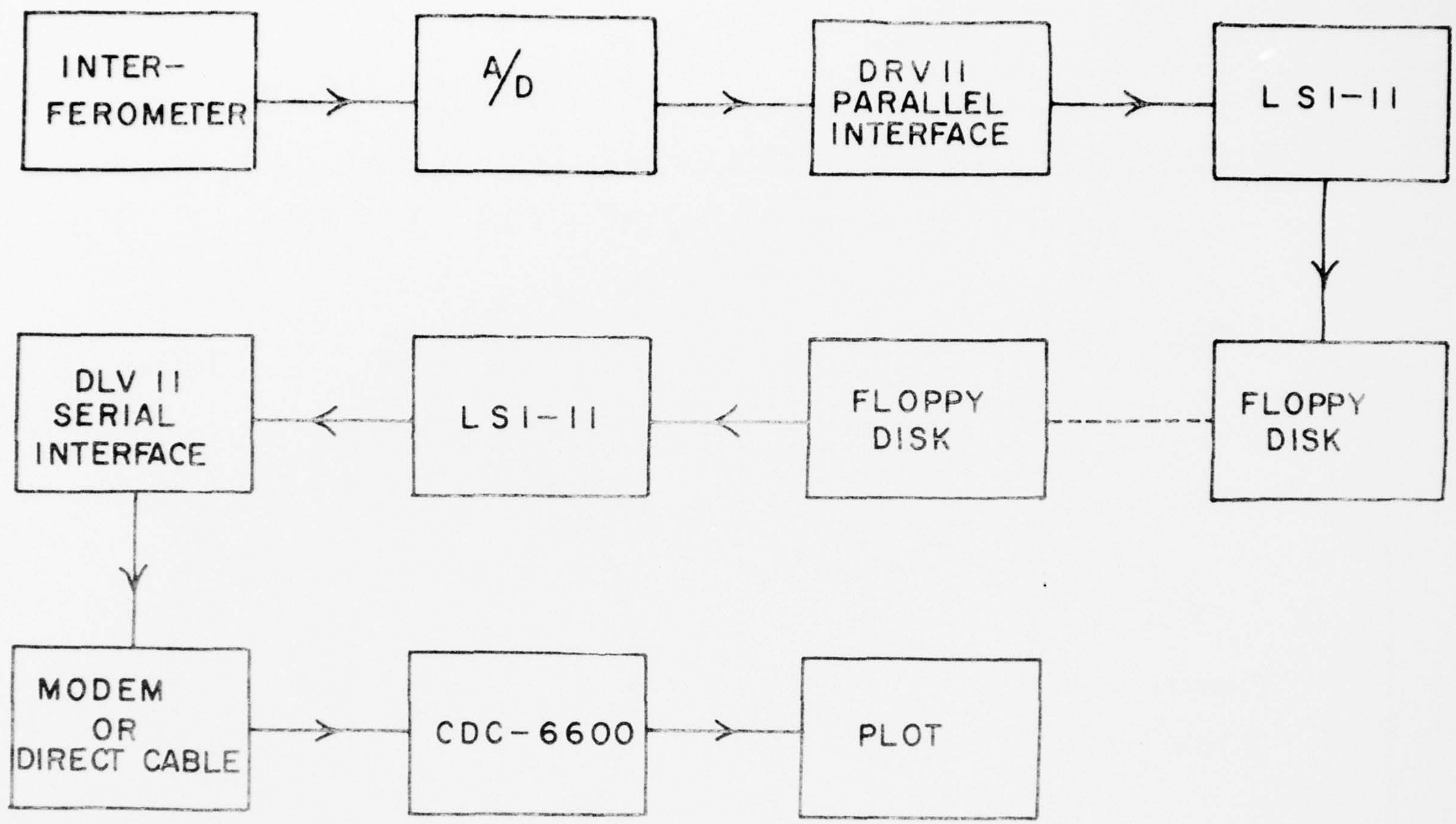

FIG. 3 DATA COLLECTION AND PROCESSING SCHEME

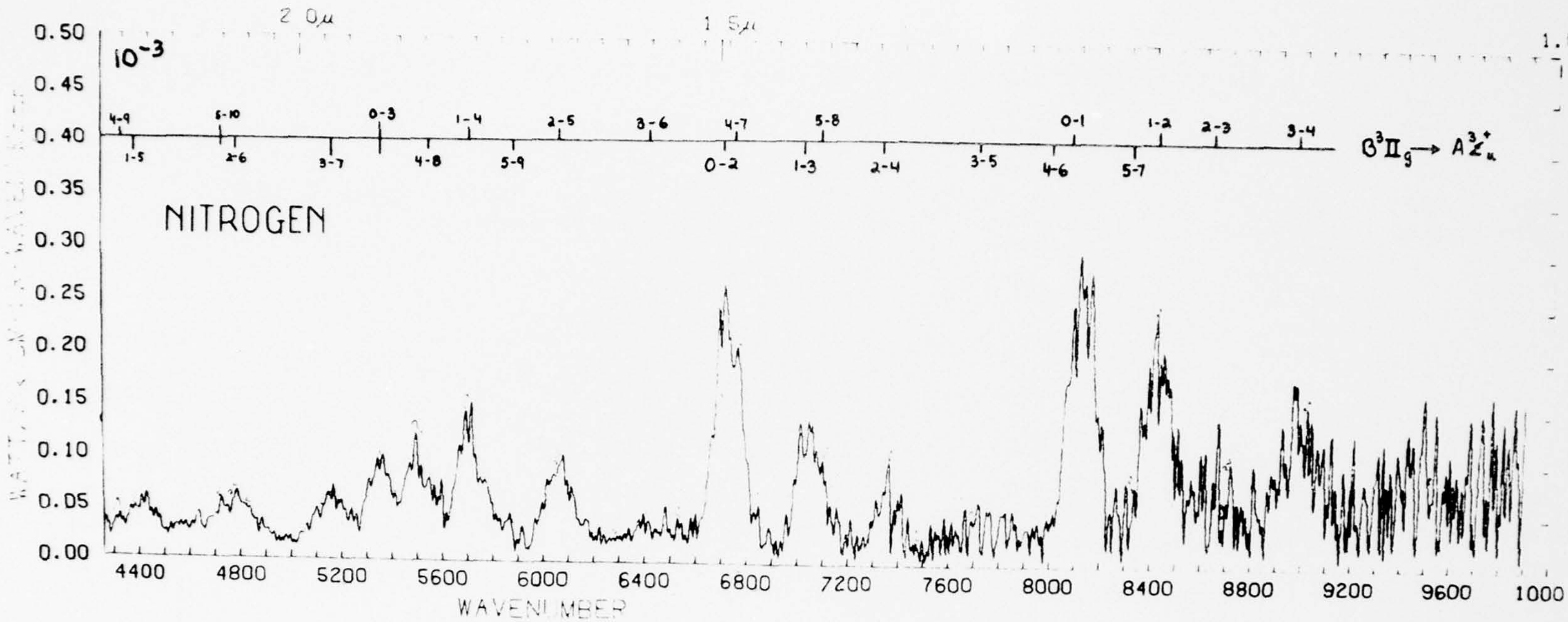

FIG. 4 EMISSION SPECTRUM OF A NITROGEN DISCHARGE

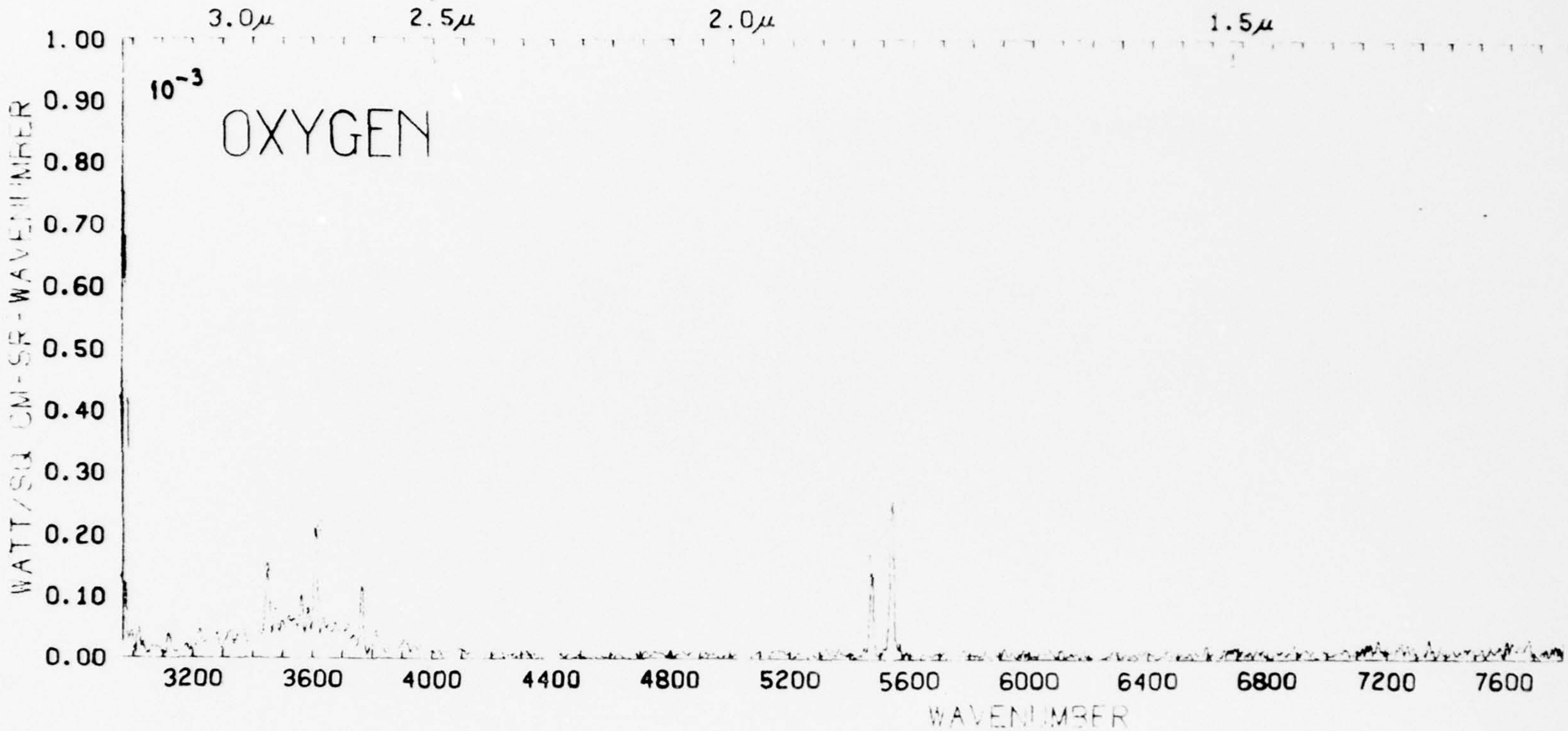

FIG. 5 EMISSION SPECTRUM OF AN OXYGEN DISCHARGE

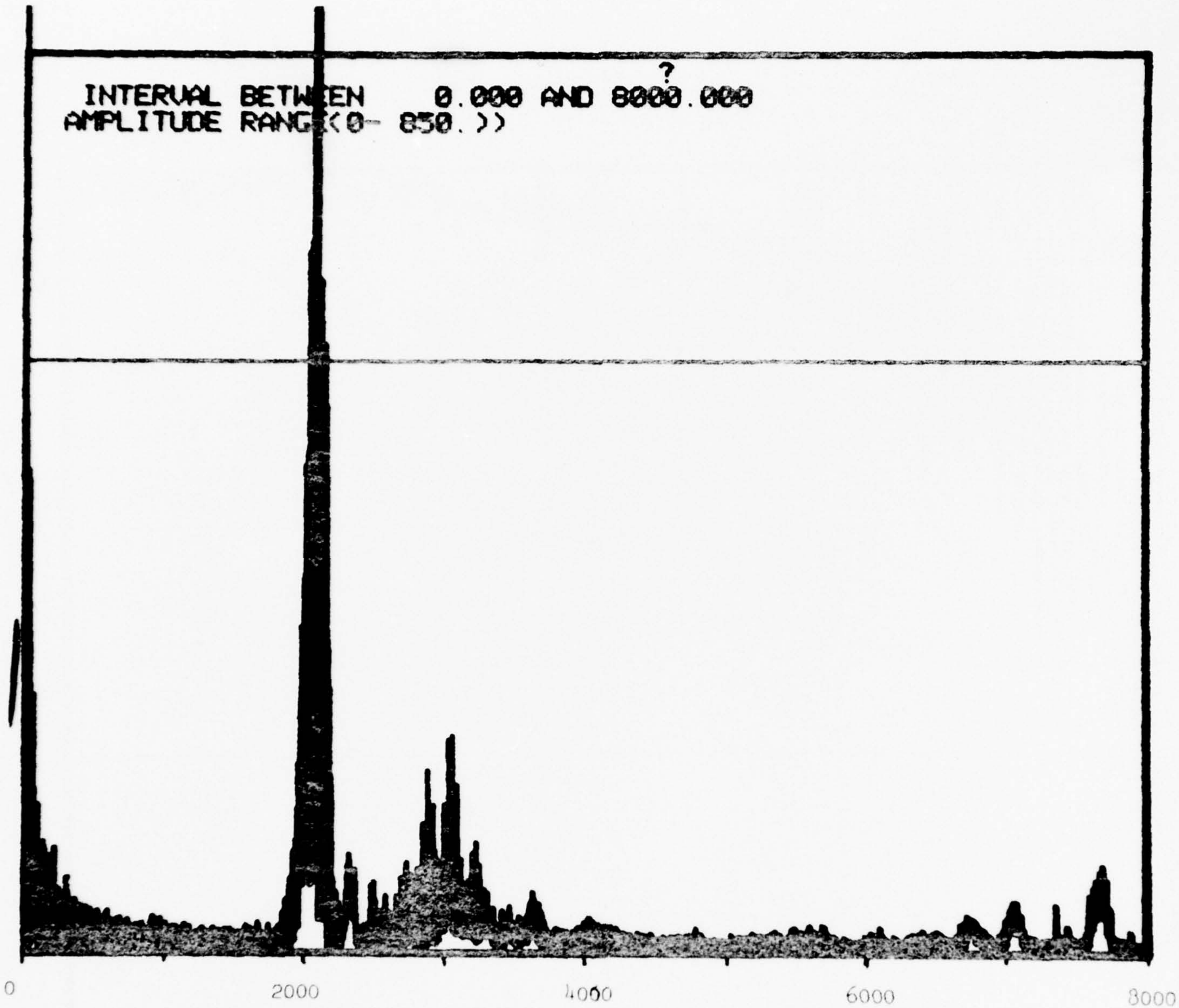
INTERVAL BETWEEN 0.000 AND 8000.000
AMPLITUDE RANGE(0- 850.))
0
2000
4000
6000
8000
Frequency (cm^{-1})

Fig. 6

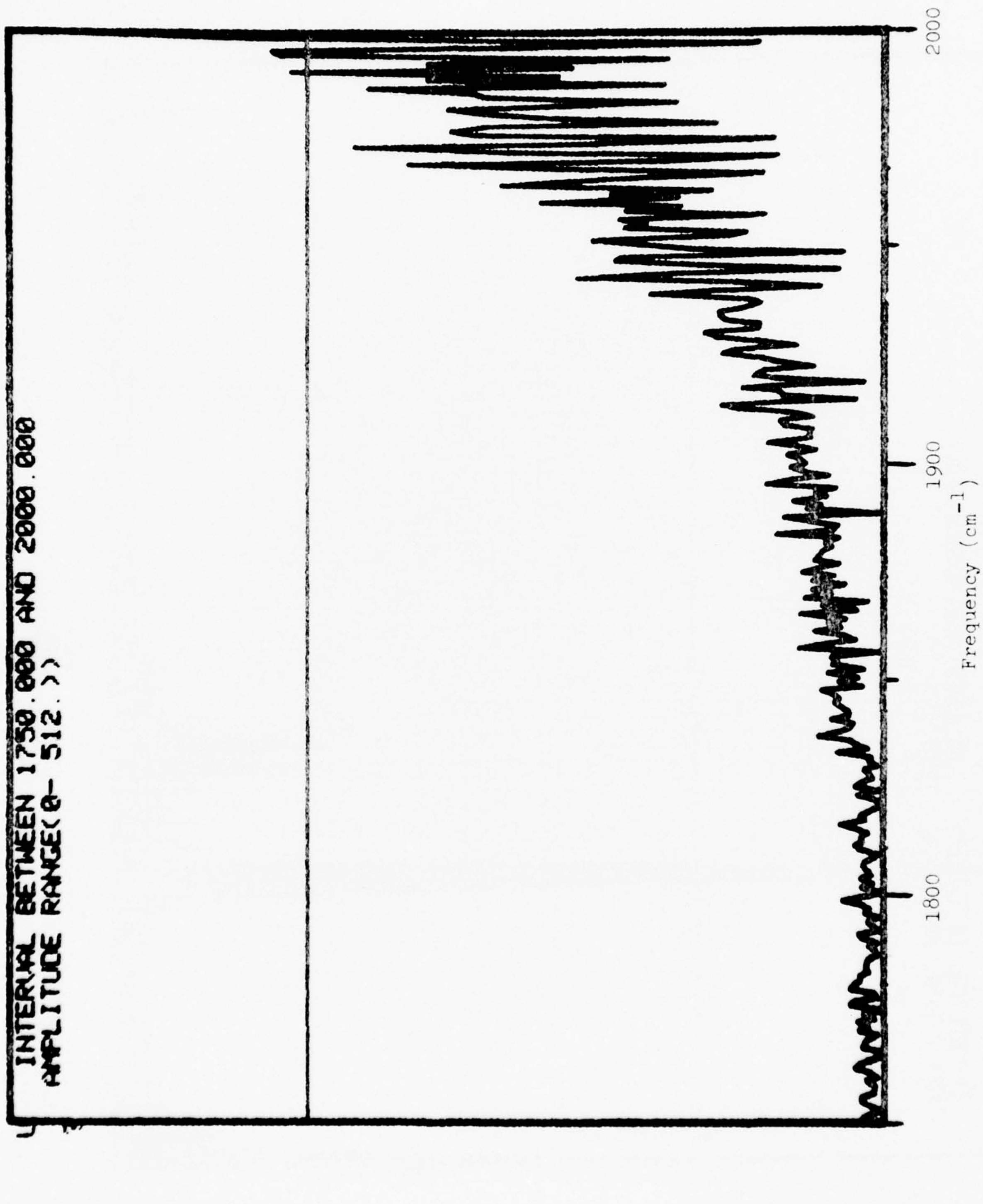
INTERVAL BETWEEN 1750.000 AND 2000.000
AMPLITUDE RANGE(0- 512.))
1800
1900
2000
Frequency (cm⁻¹)

Fig. 7

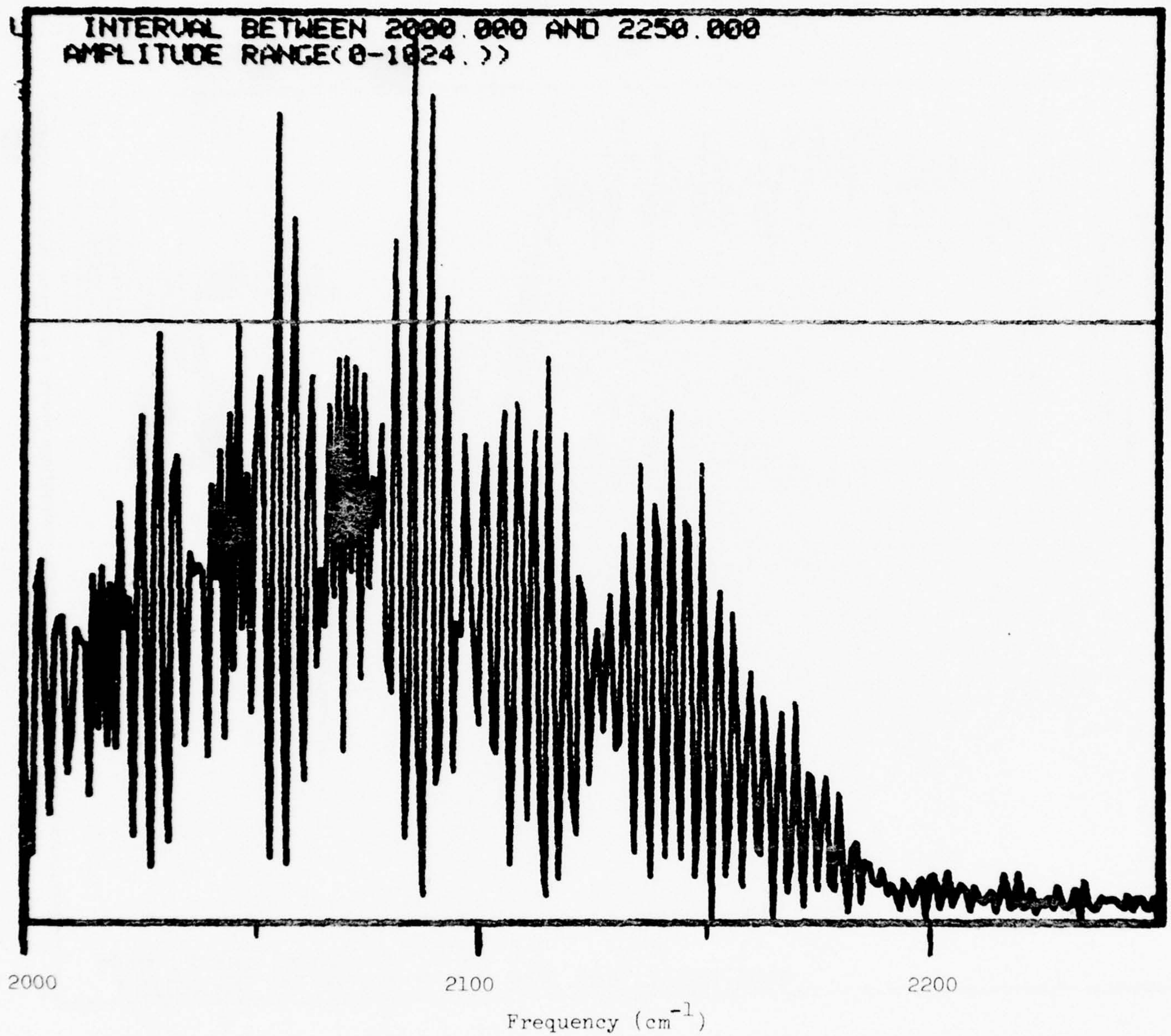
INTERVAL BETWEEN 2000.000 AND 2250.000
AMPLITUDE RANGE(0-1024.))
2000
2100
2200
Frequency (cm^{-1})

Fig. 8

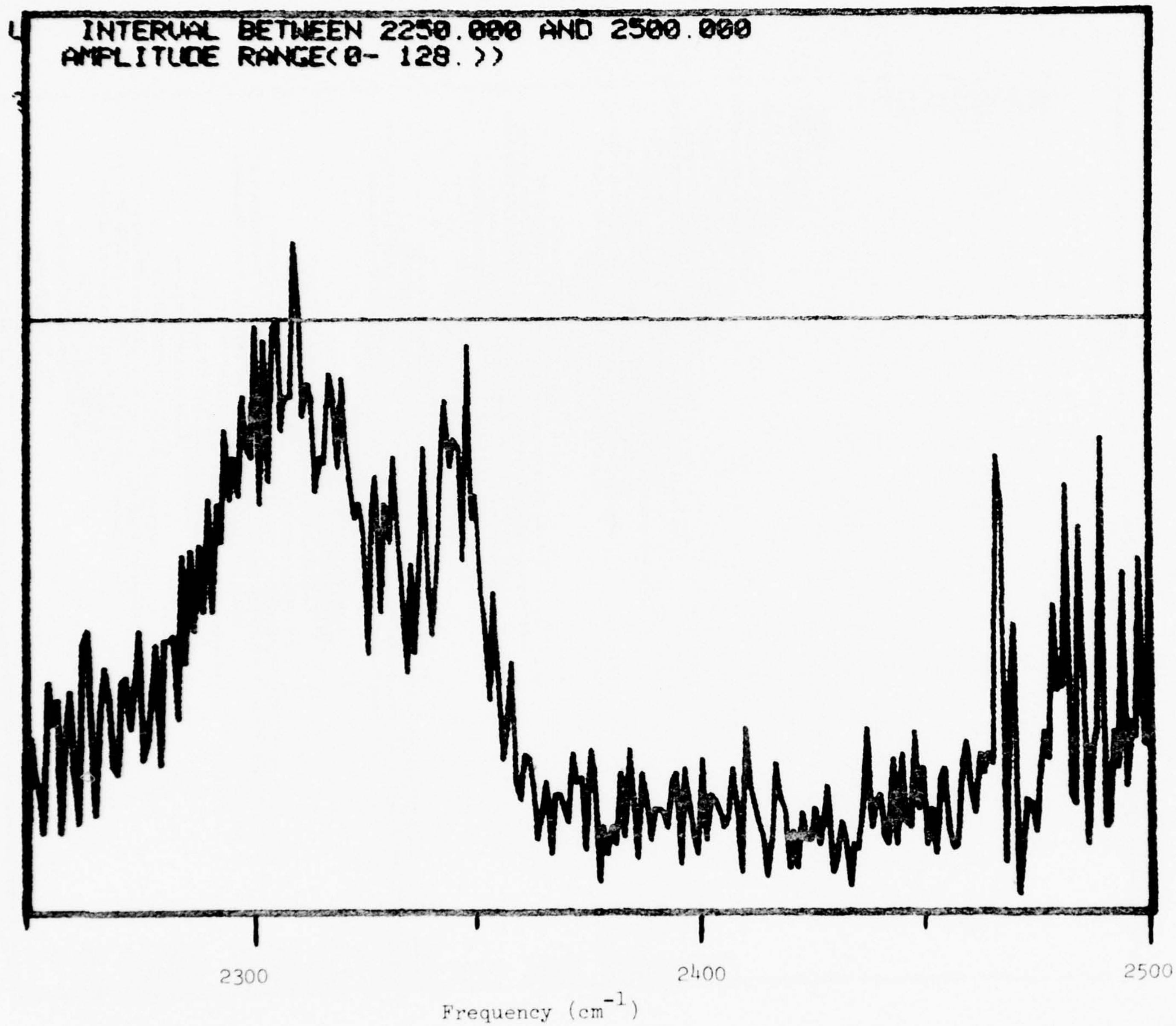
INTERVAL BETWEEN 2250.000 AND 2500.000
AMPLITUDE RANGE(0- 128.))
2300
2400
2500
Frequency (cm^{-1})

Fig. 9

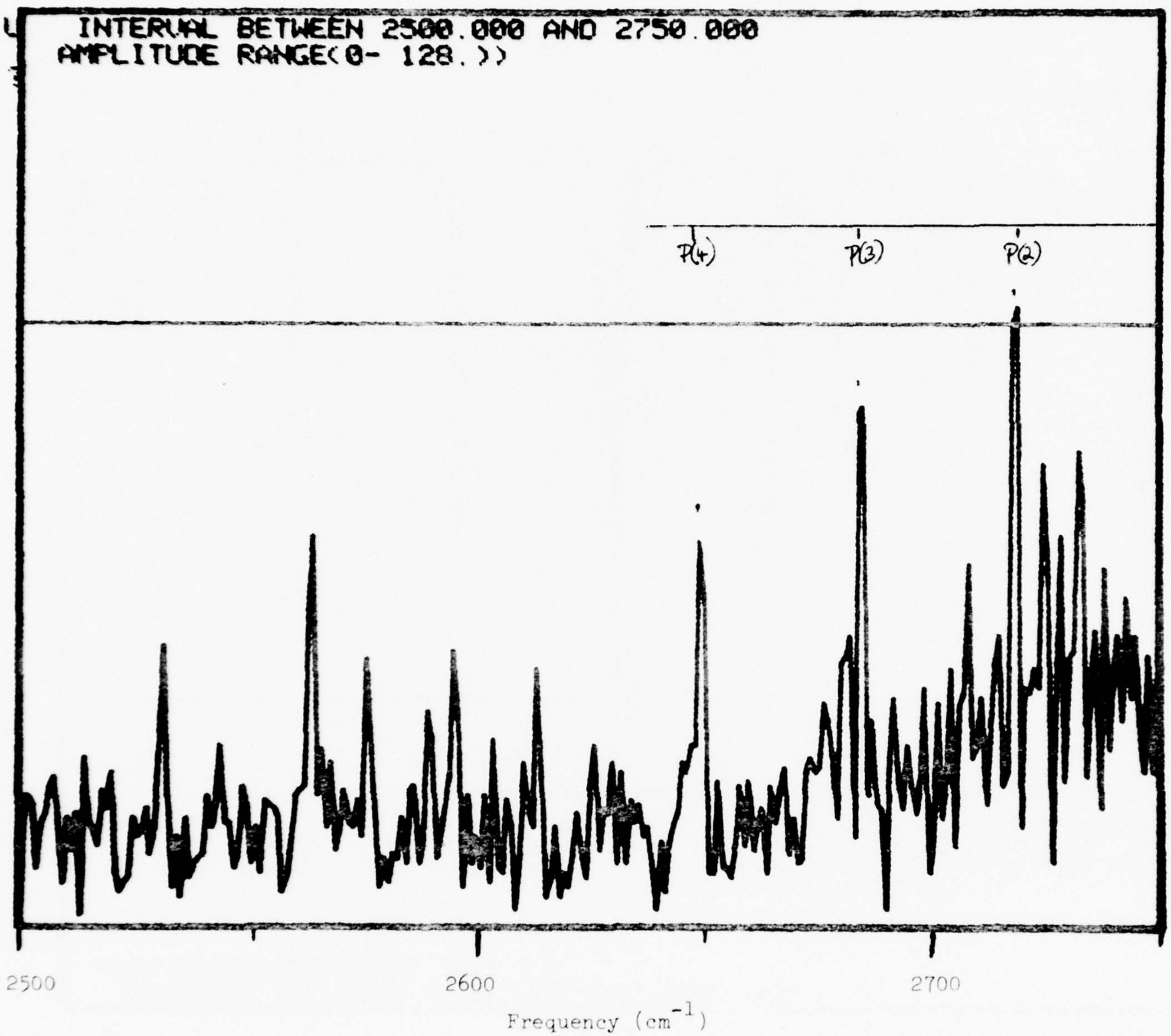
INTERVAL BETWEEN 2500.000 AND 2750.000
AMPLITUDE RANGE(0- 128.))
P(4)
P(3)
P(2)
2500
2600
2700
Frequency (cm^{-1})

Fig. 10

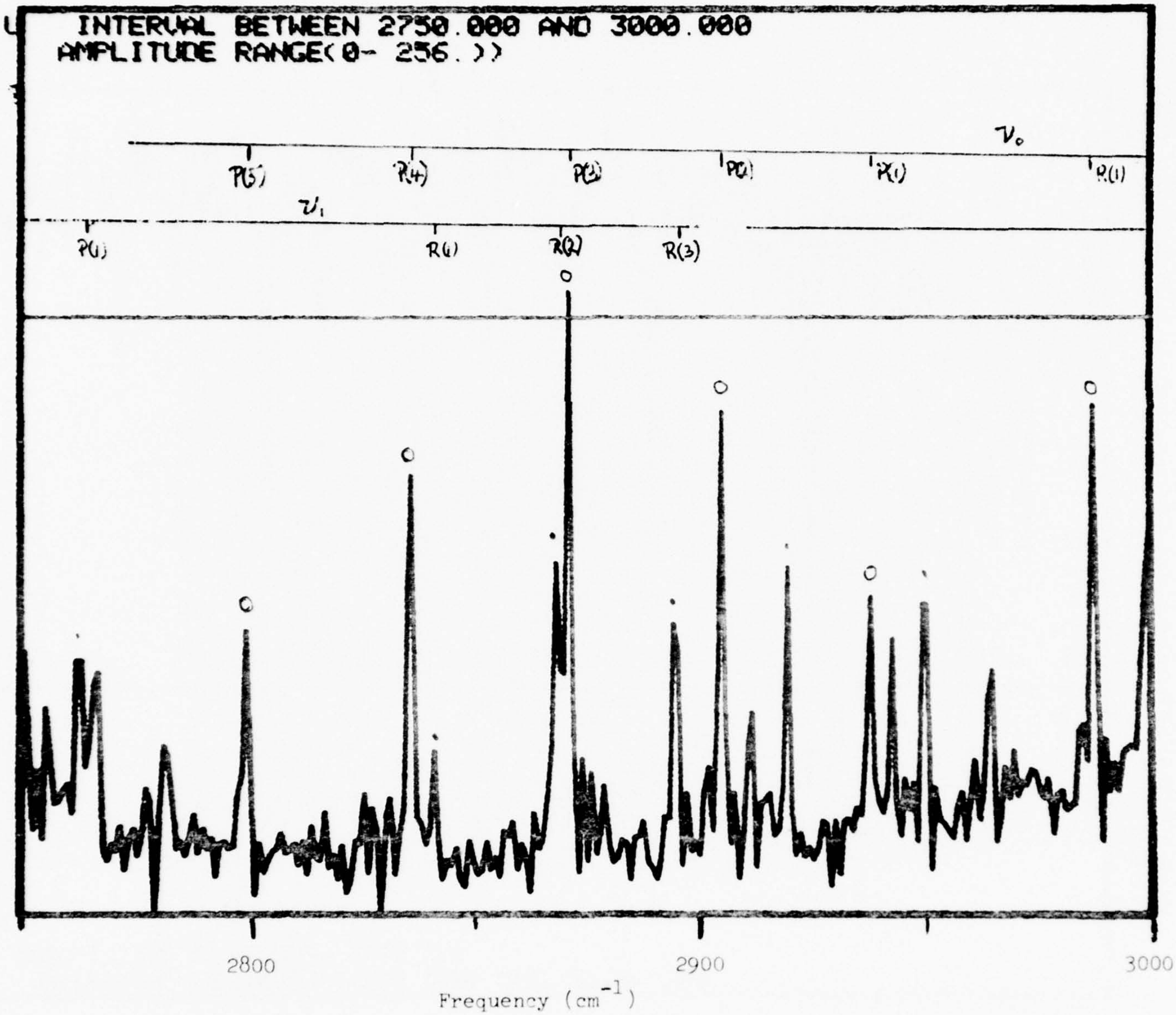
INTERVAL BETWEEN 2750.000 AND 3000.000
AMPLITUDE RANGE(0- 256.))
ν_0
P(5)
P(4)
P(3)
P(2)
P(1)
R(1)
ν_1
P(1)
R(1)
R(2)
R(3)
2800
2900
3000
Frequency (cm^{-1})

Fig. 11

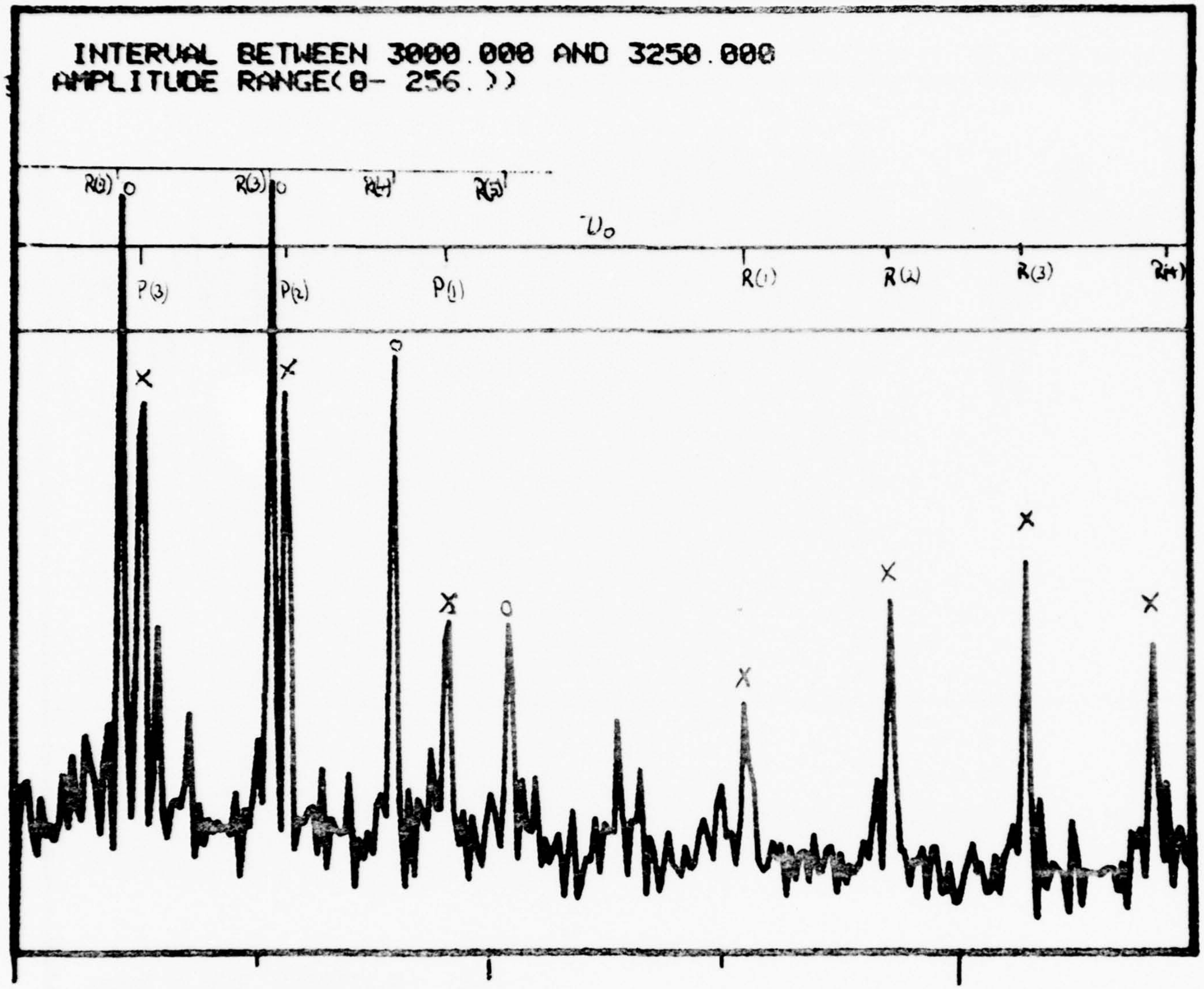
INTERVAL BETWEEN 3000.000 AND 3250.000
AMPLITUDE RANGE(0- 256.))
R(3)
R(3)
R(4)
R(5)
ν_0
P(3)
P(2)
P(1)
R(1)
R(2)
R(3)
R(4)
3000
3100
3200
Frequency (cm^{-1})

Fig. 12

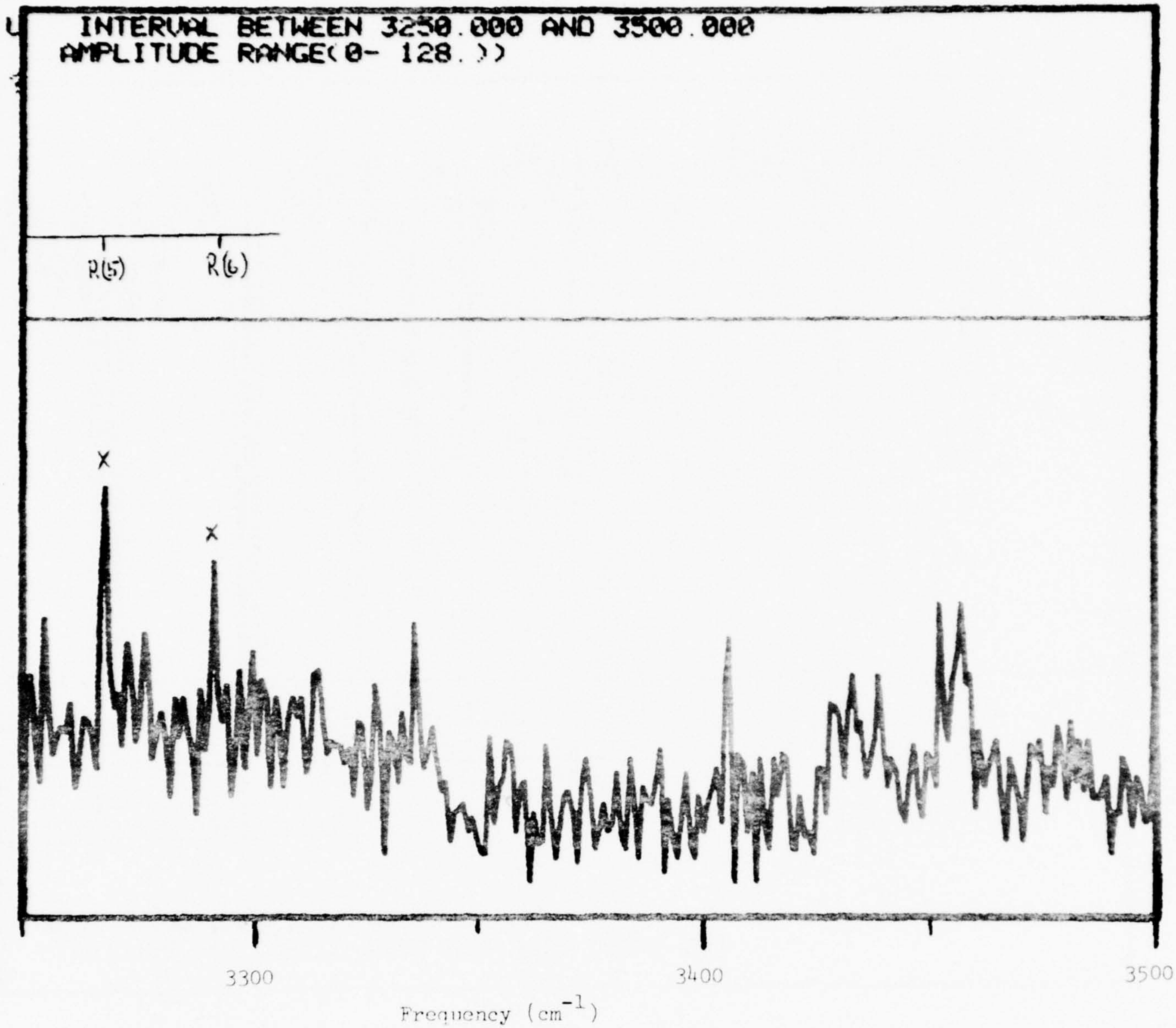
INTERVAL BETWEEN 3250.000 AND 3500.000
AMPLITUDE RANGE(0- 128.))
R(5)
R(6)
X
X
3300
3400
3500
Frequency (cm^{-1})

Fig. 13

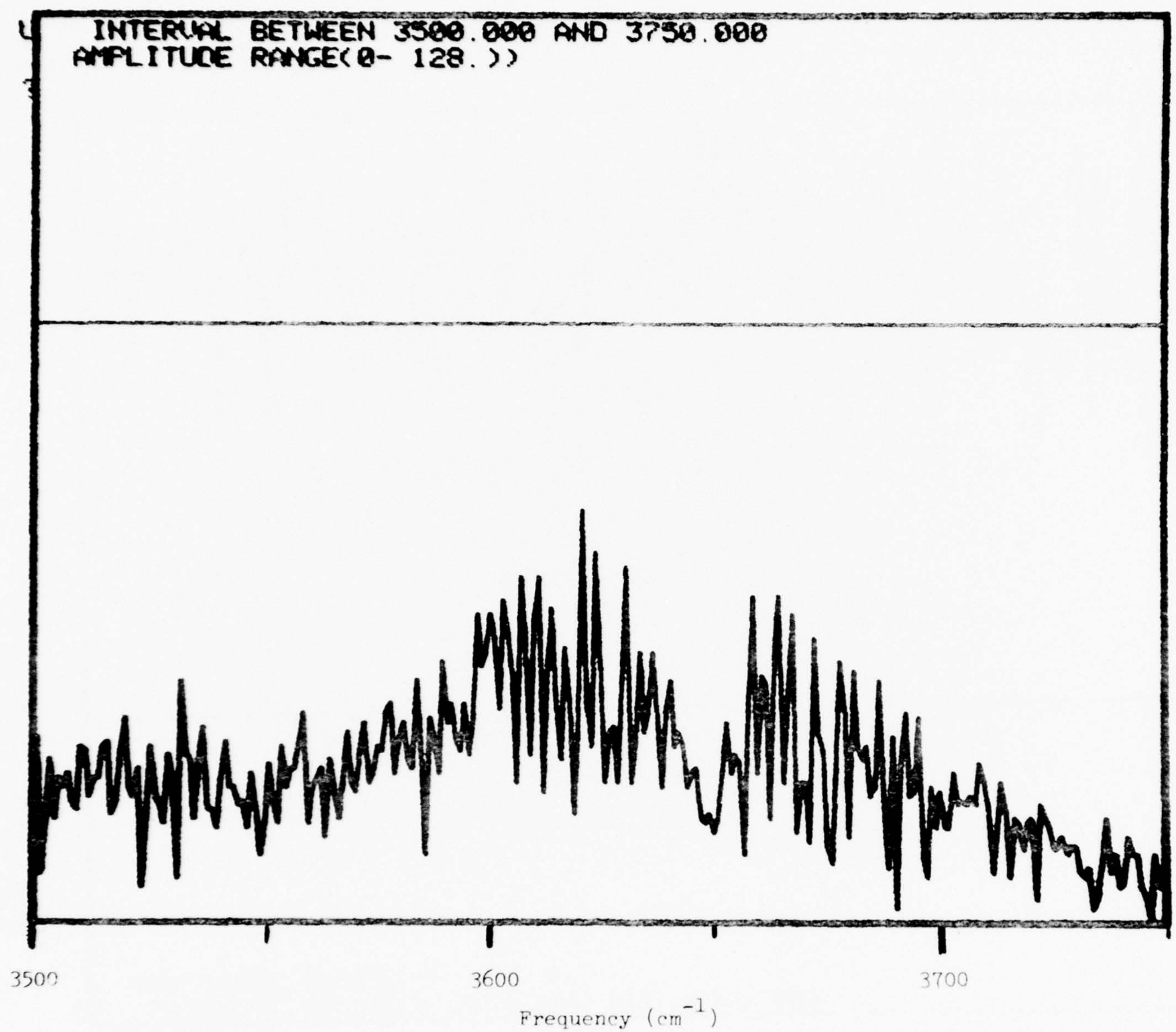
INTERVAL BETWEEN 3500.000 AND 3750.000
AMPLITUDE RANGE(0- 128.))
3500
3600
3700
Frequency (cm^{-1})

Fig. 14

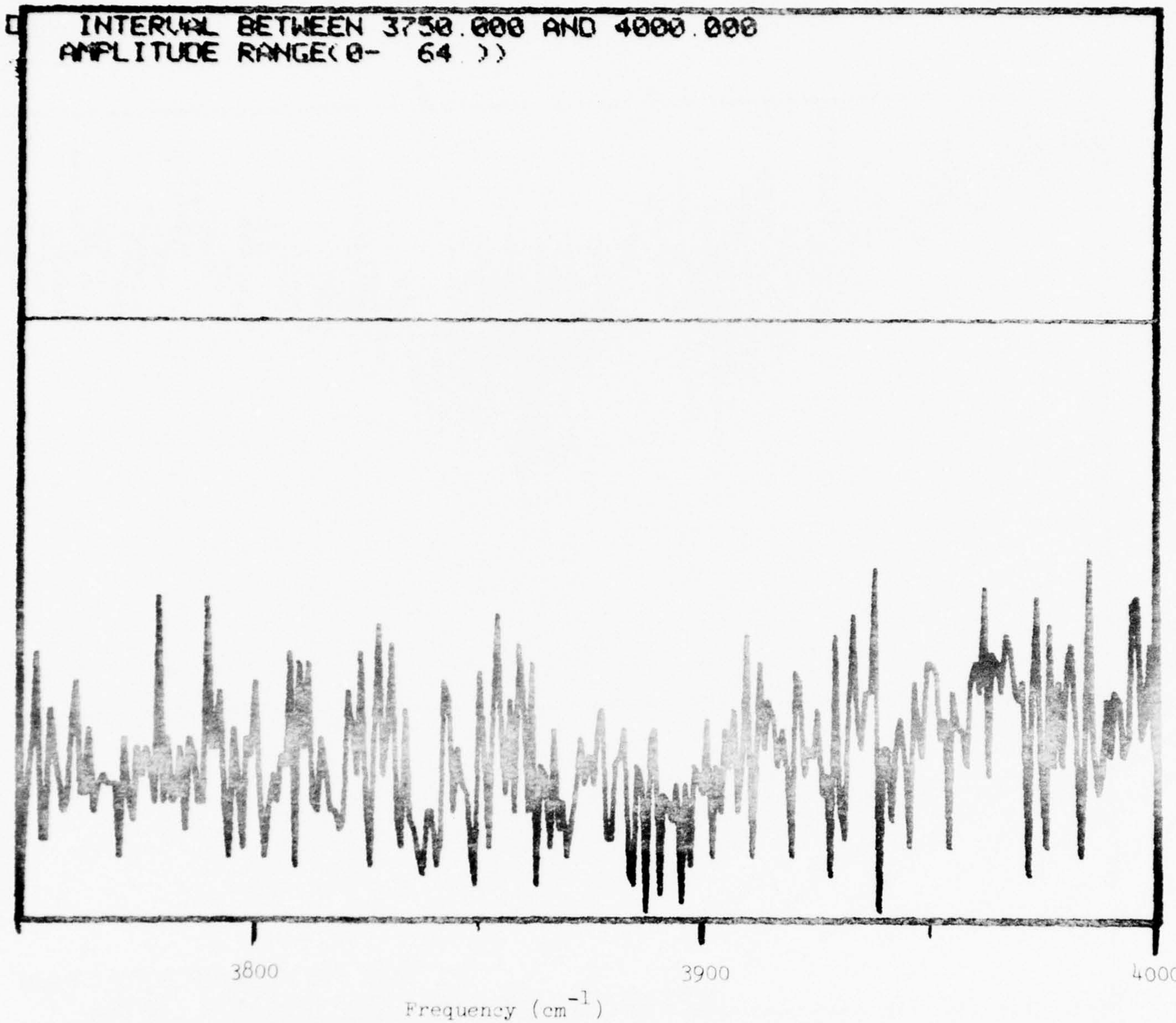
INTERVAL BETWEEN 3750.000 AND 4000.000
AMPLITUDE RANGE(0- 64))
3800
3900
4000
Frequency (cm^{-1})

Fig. 15

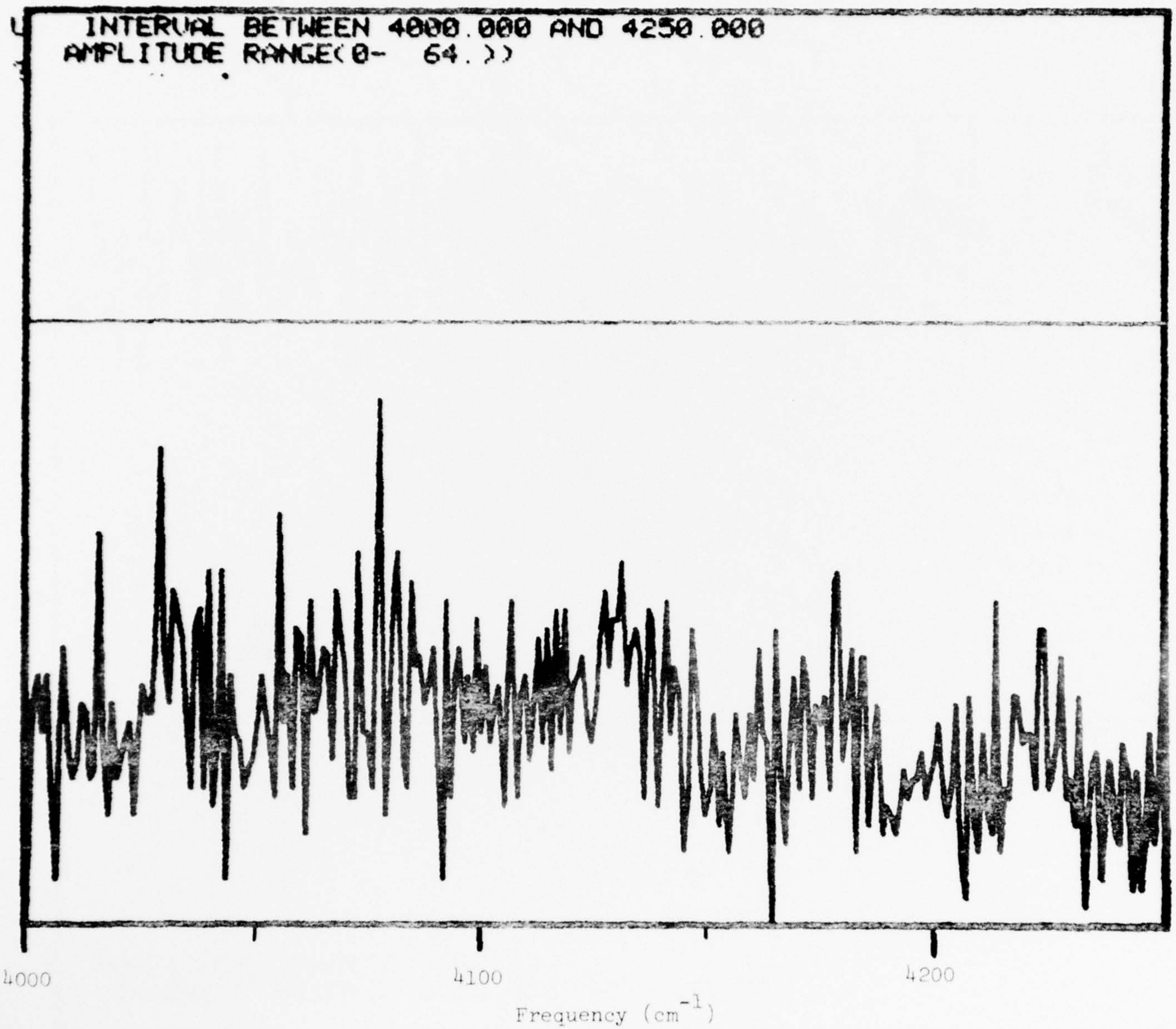
INTERVAL BETWEEN 4000.000 AND 4250.000
AMPLITUDE RANGE(0- 64.))
4000
4100
4200
Frequency (cm^{-1})

Fig. 16

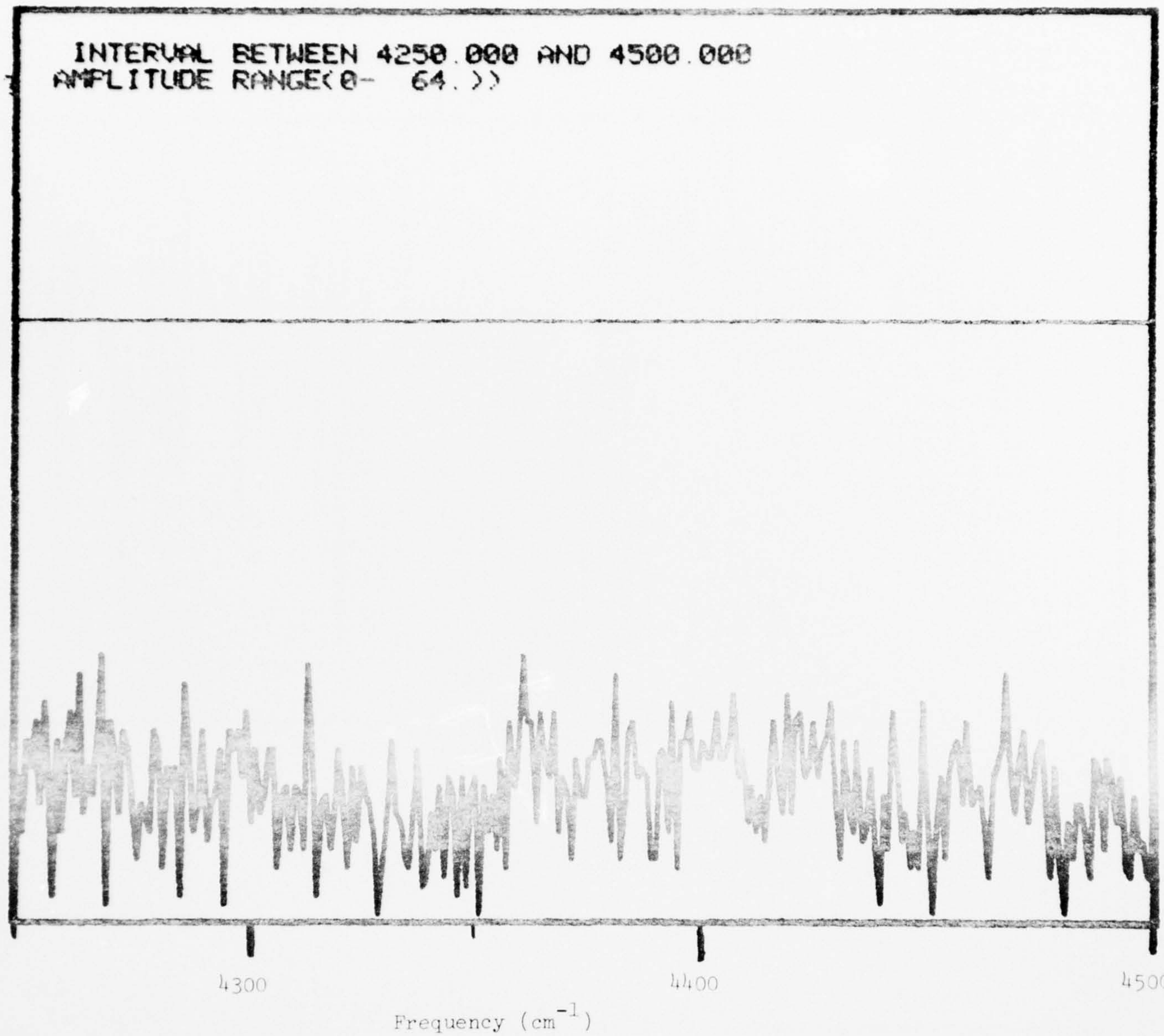
INTERVAL BETWEEN 4250.000 AND 4500.000
AMPLITUDE RANGE(0- 64.))
4300
4400
4500
Frequency (cm^{-1})

Fig. 17

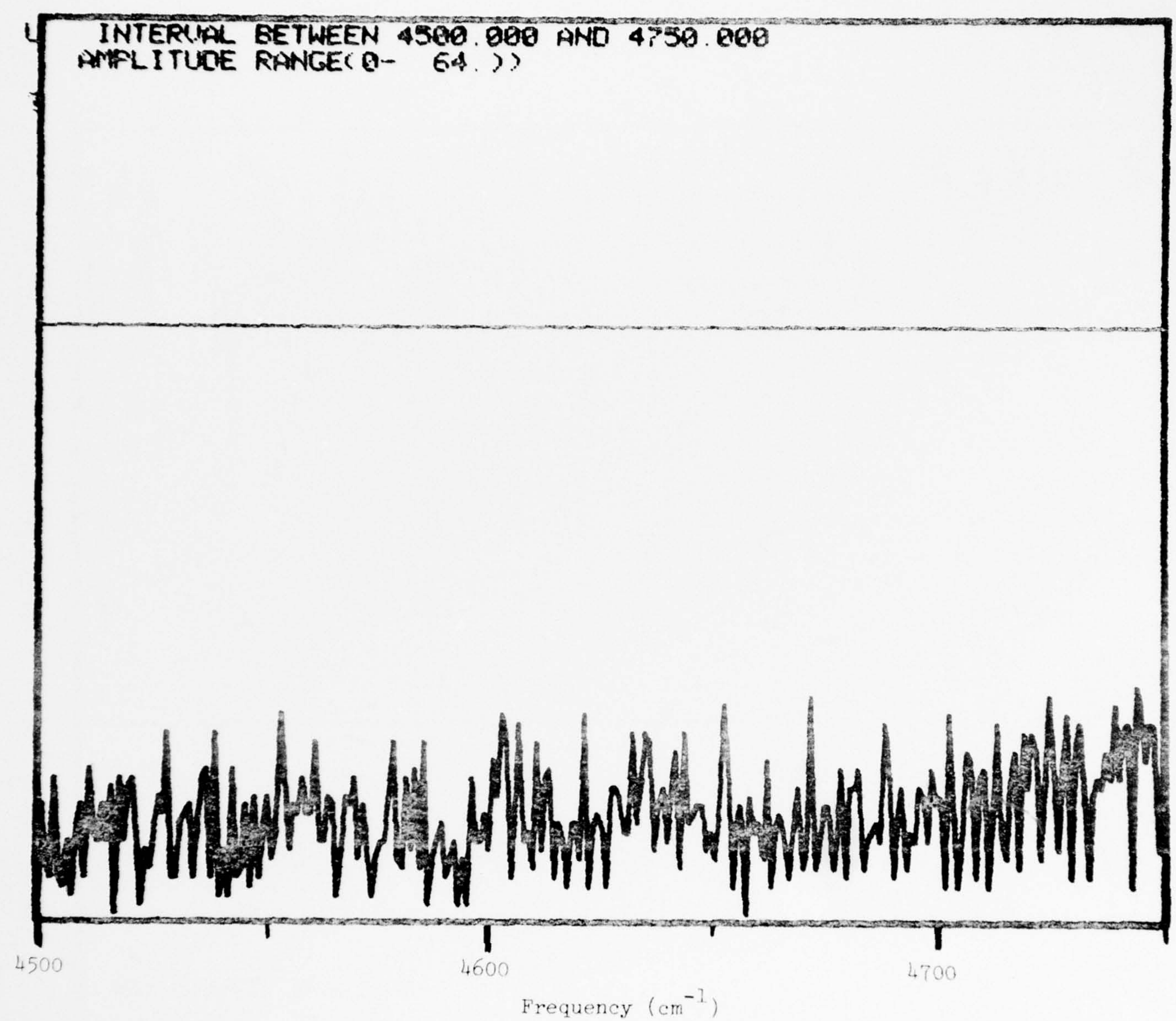
INTERVAL BETWEEN 4500.000 AND 4750.000
AMPLITUDE RANGE(0- 64.))
4500
4600
4700
Frequency (cm^{-1})

Fig. 18

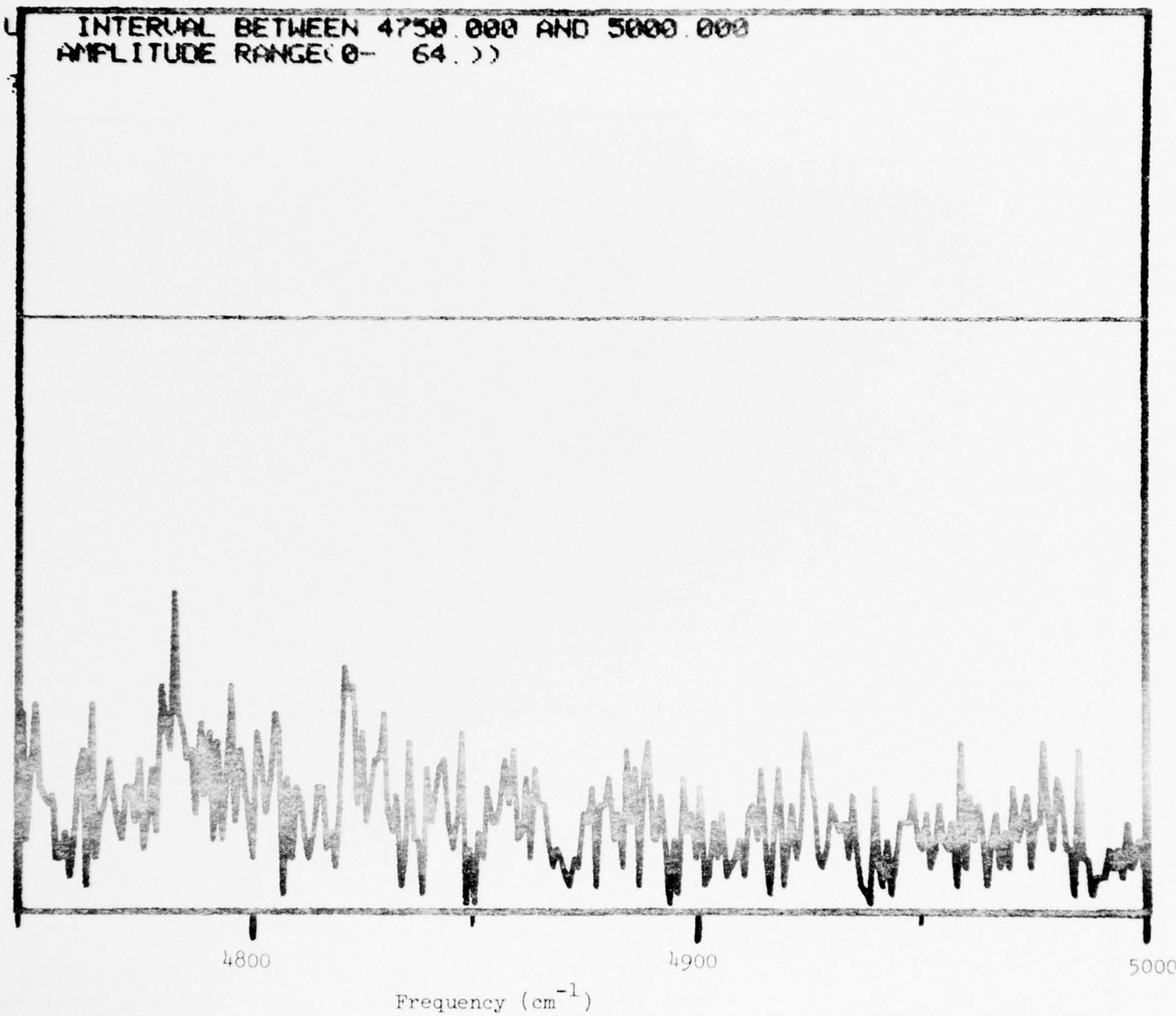
INTERVAL BETWEEN 4750.000 AND 5000.000
AMPLITUDE RANGE(0- 64.))
4800
4900
5000
Frequency (cm-1)

Fig. 19

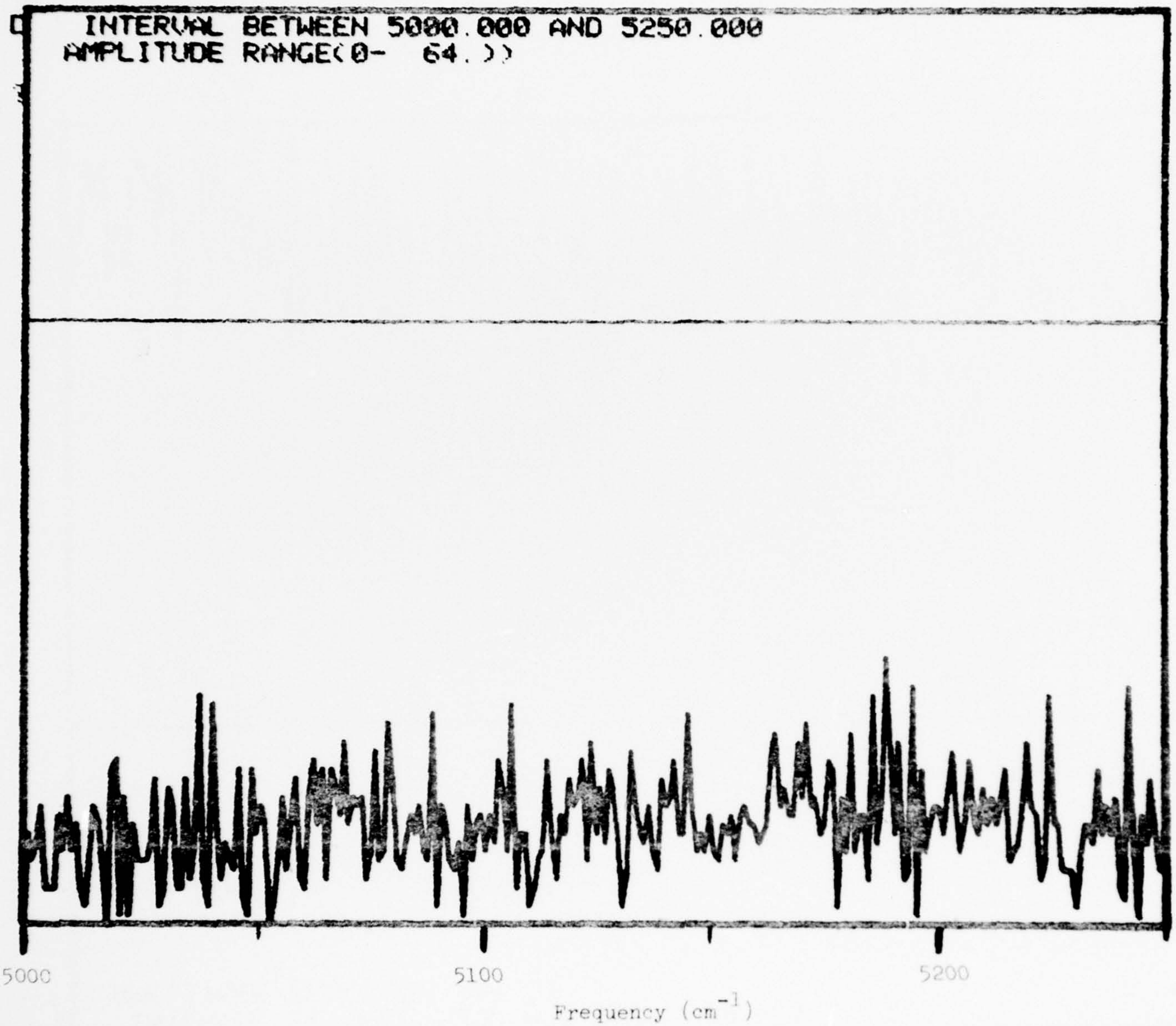

INTERVAL BETWEEN 5000.000 AND 5250.000
AMPLITUDE RANGE(0- 64.))
5000
5100
5200
Frequency (cm^-1)

Fig. 20

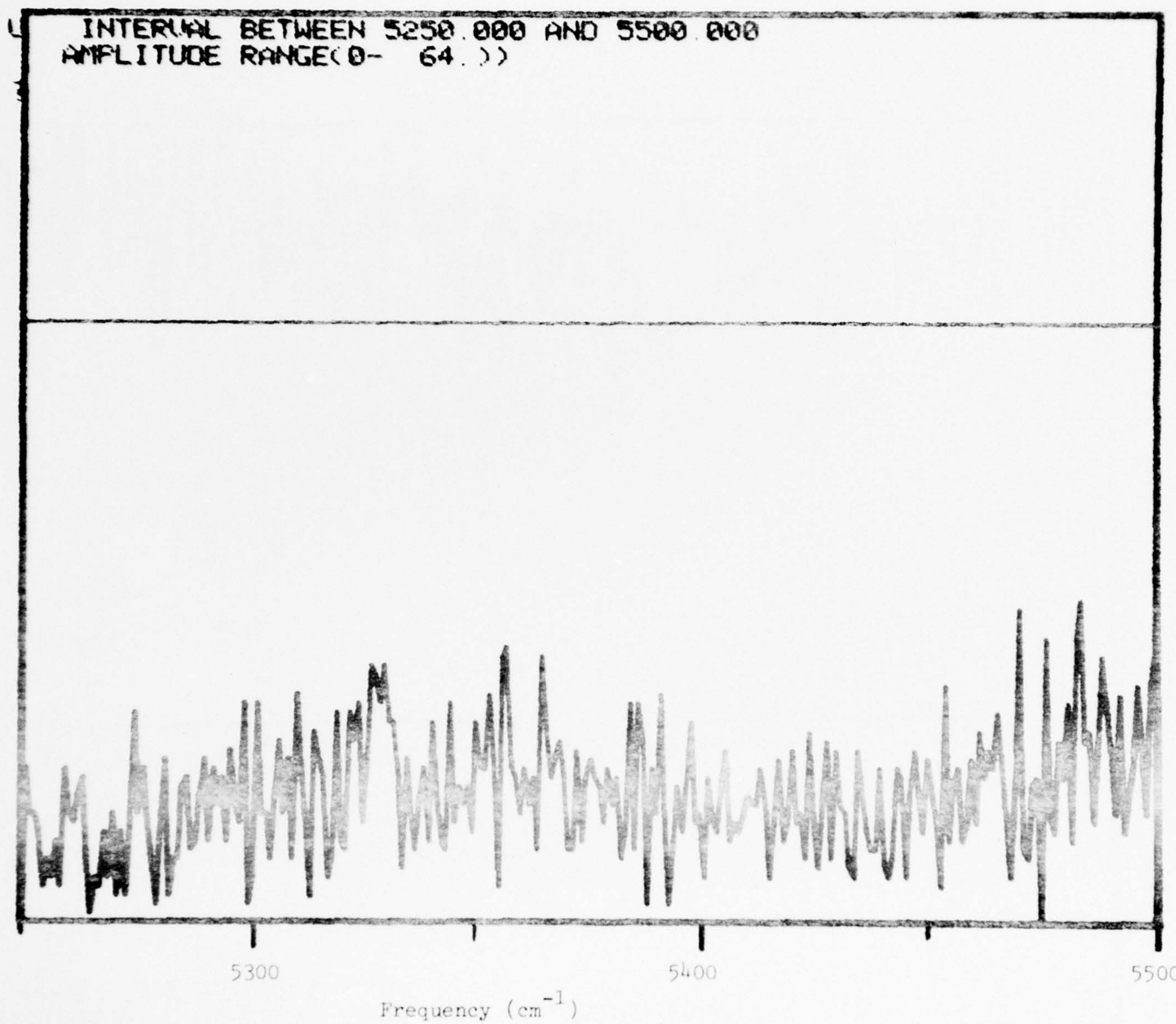
INTERVAL BETWEEN 5250.000 AND 5500.000
AMPLITUDE RANGE(0- 64.))
5300
5400
5500
Frequency (cm^{-1})

Fig. 21

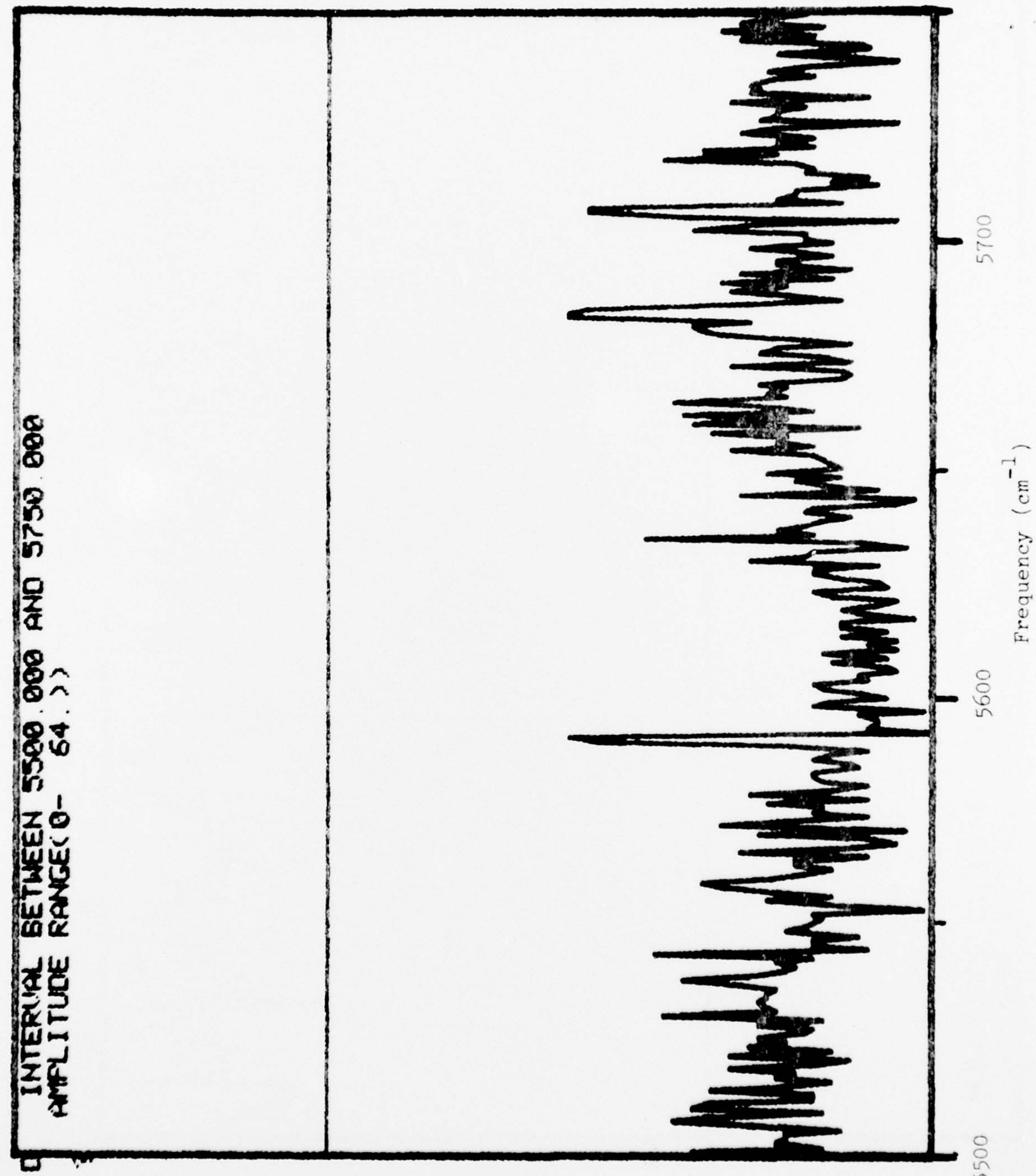

INTERVAL BETWEEN 5500.000 AND 5750.000
AMPLITUDE RANGE(0- 64.))
5500
5600
5700
Frequency (cm^{-1})

Fig. 22

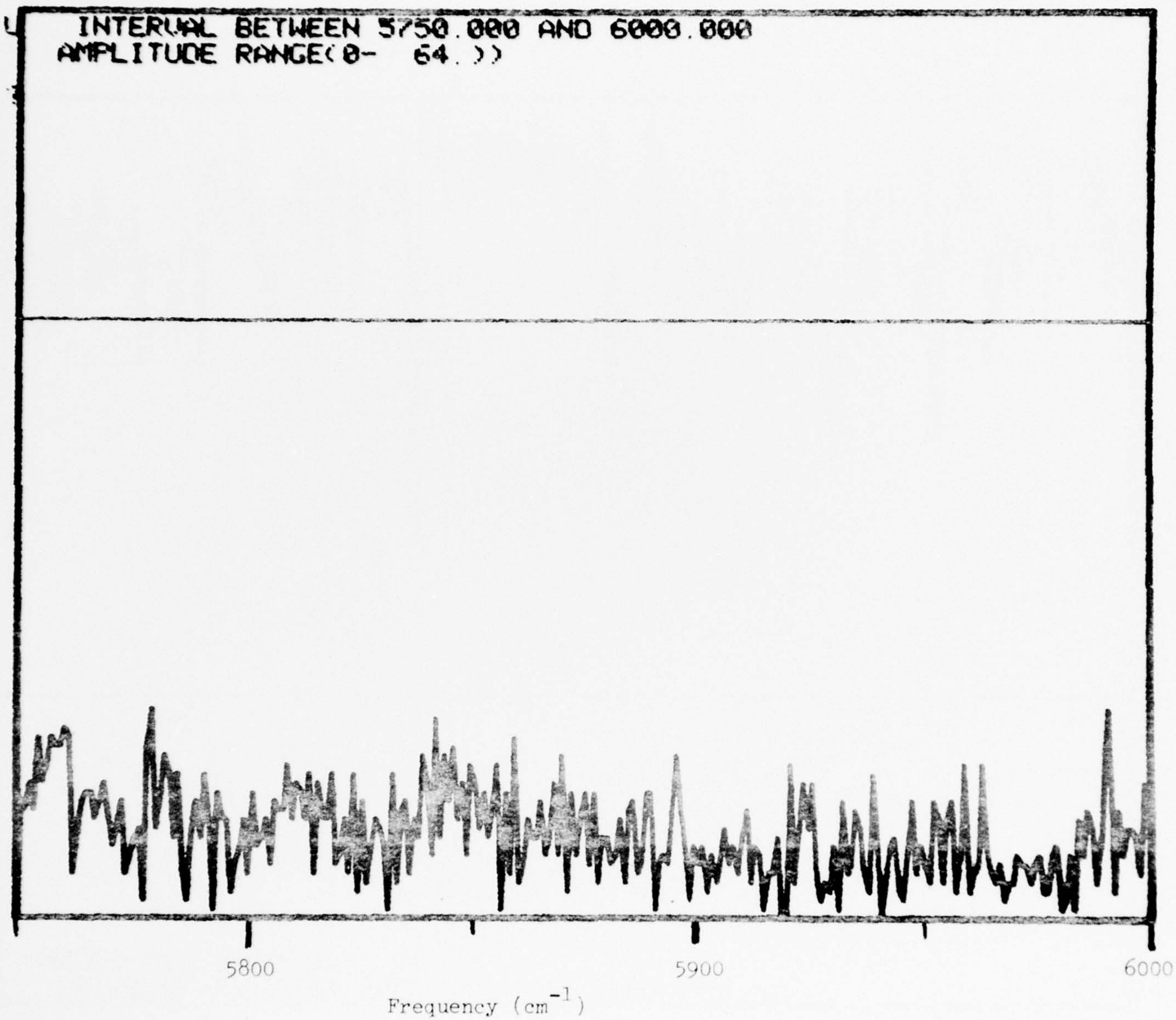

INTERVAL BETWEEN 5750.000 AND 6000.000
AMPLITUDE RANGE(0- 64.))
5800
5900
6000
Frequency (cm-1)

Fig. 23

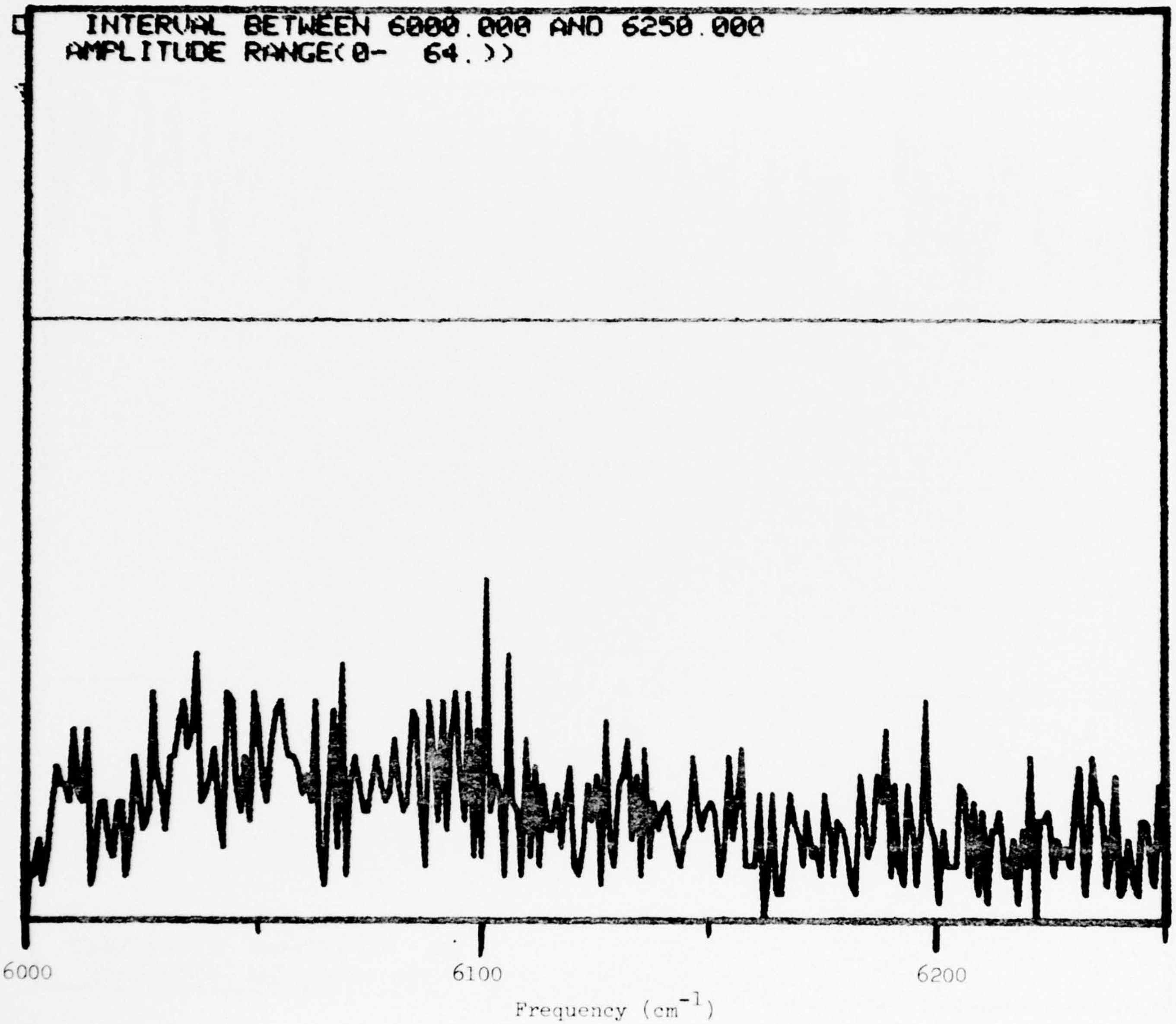
INTERVAL BETWEEN 6000.000 AND 6250.000
AMPLITUDE RANGE(0- 64.))
6000
6100
6200
Frequency (cm^-1)

Fig. 24

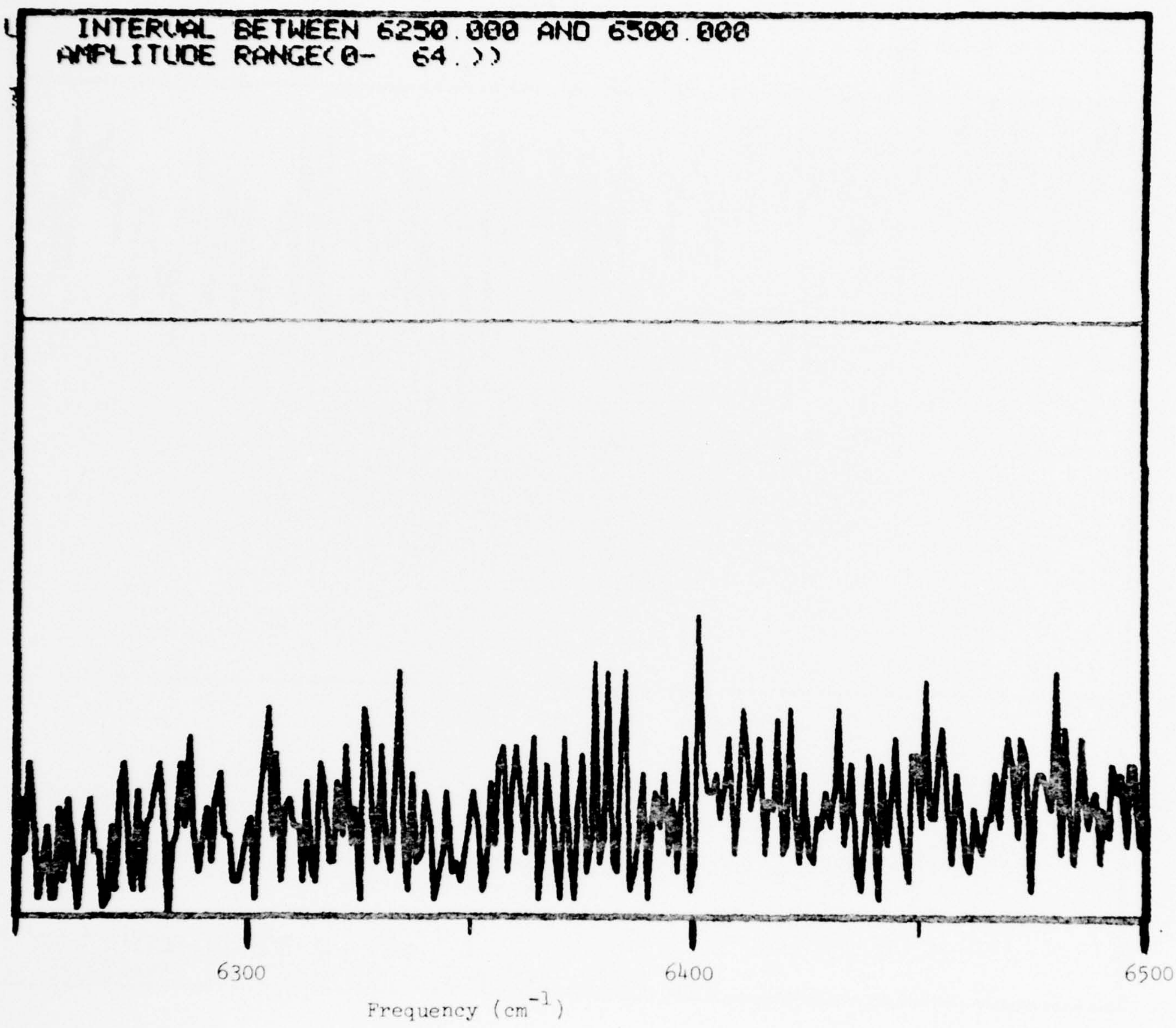
INTERVAL BETWEEN 6250.000 AND 6500.000
AMPLITUDE RANGE(0- 64.))
6300
6400
6500
Frequency (cm^{-1})

Fig. 25

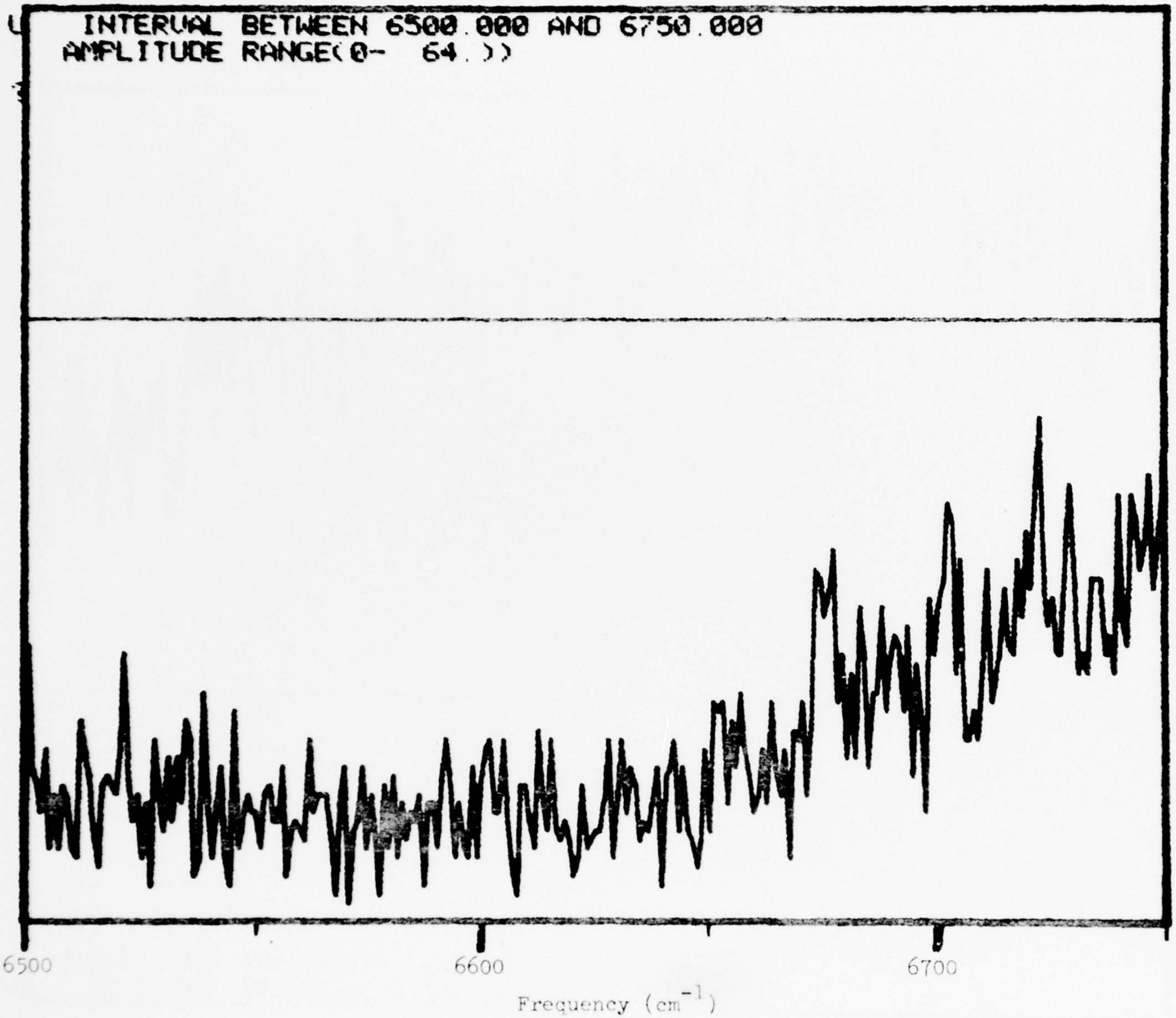

INTERVAL BETWEEN 6500.000 AND 6750.000
AMPLITUDE RANGE(0- 64.))
6500
6600
6700
Frequency (cm-1)

Fig. 26

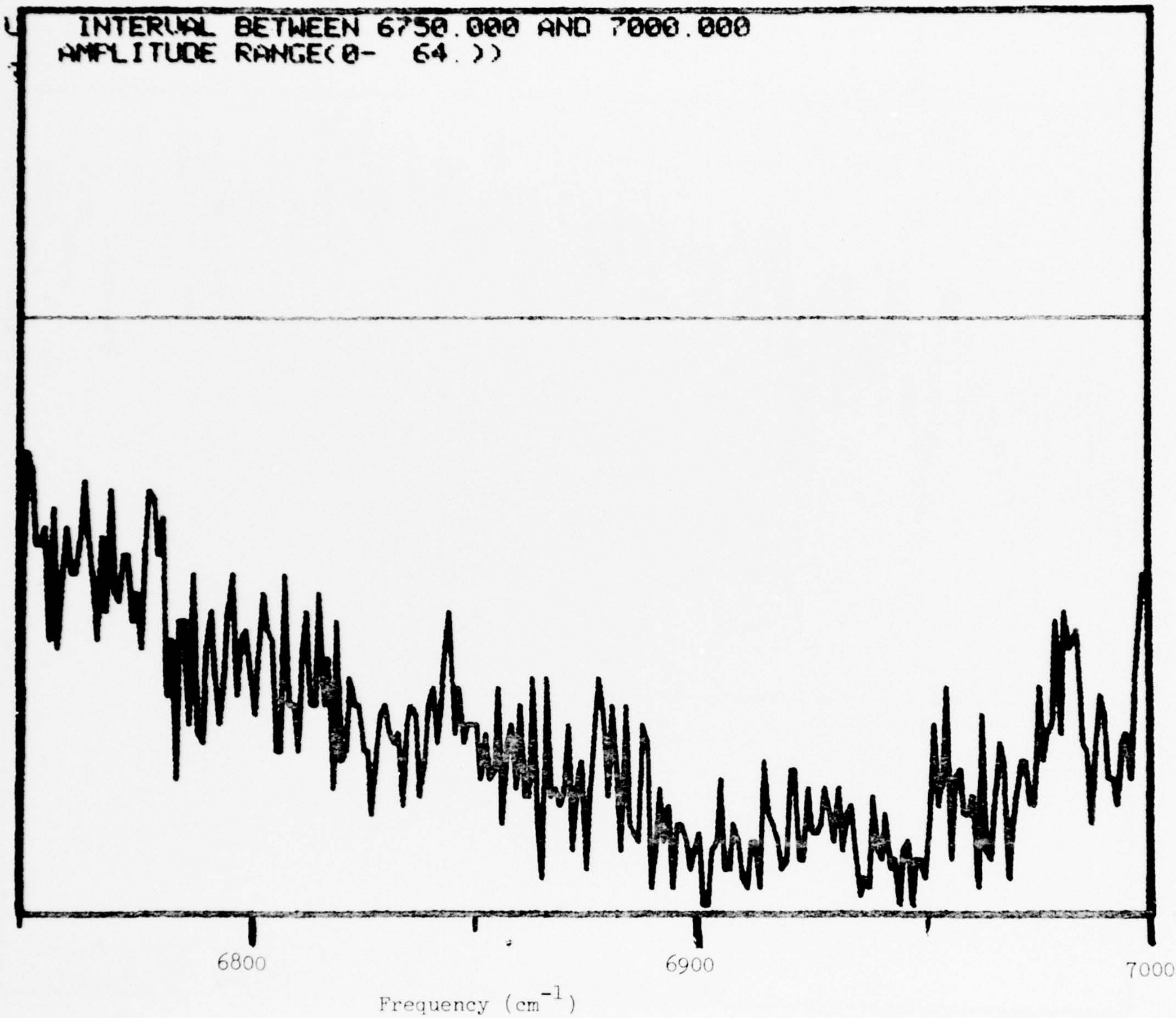

INTERVAL BETWEEN 6750.000 AND 7000.000
AMPLITUDE RANGE(0-   64.))
6800
6900
7000
Frequency (cm-1)

Fig. 27

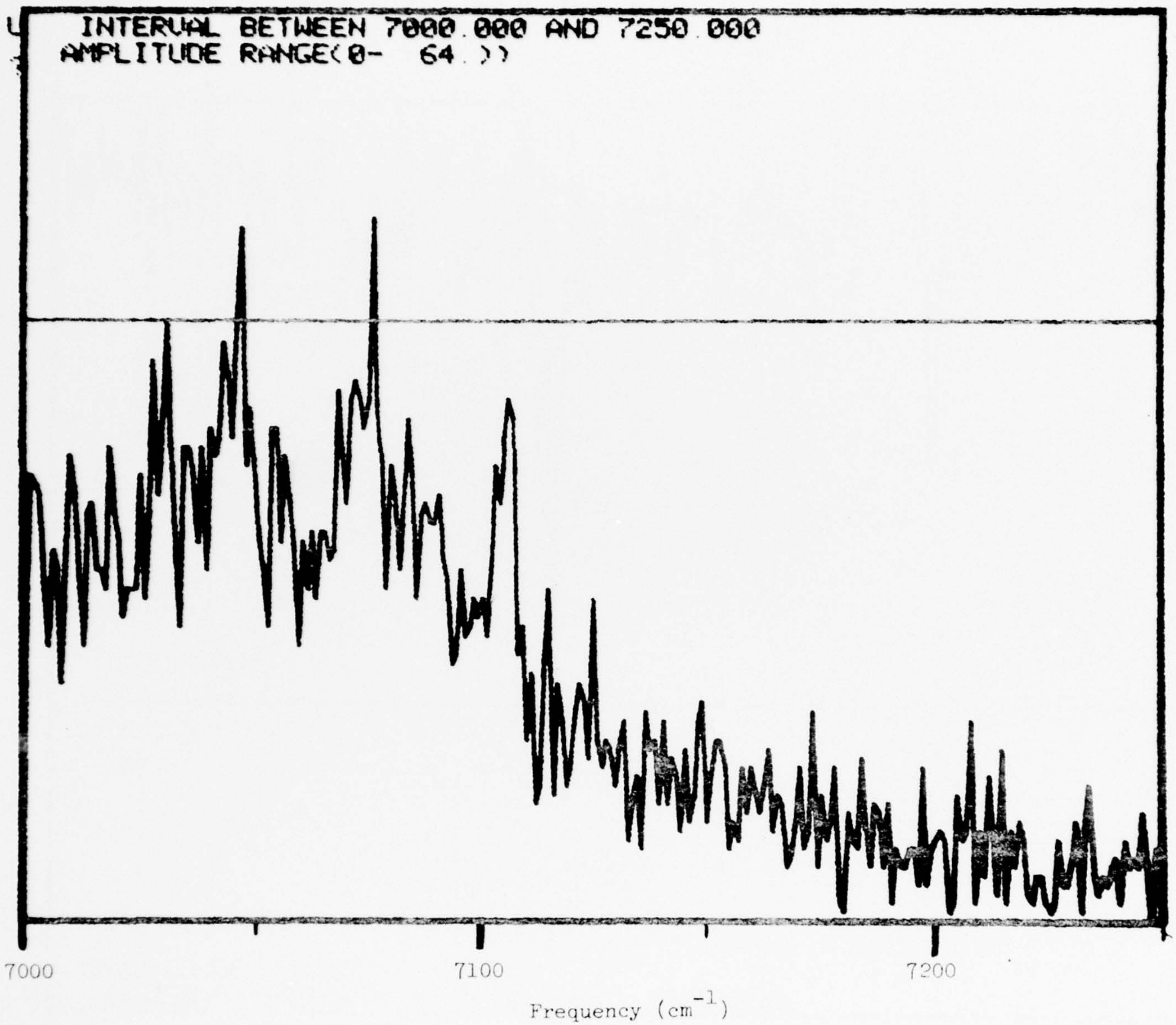
INTERVAL BETWEEN 7000.000 AND 7250.000
AMPLITUDE RANGE(0- 64.))
7000
7100
7200
Frequency (cm^{-1})

Fig. 28

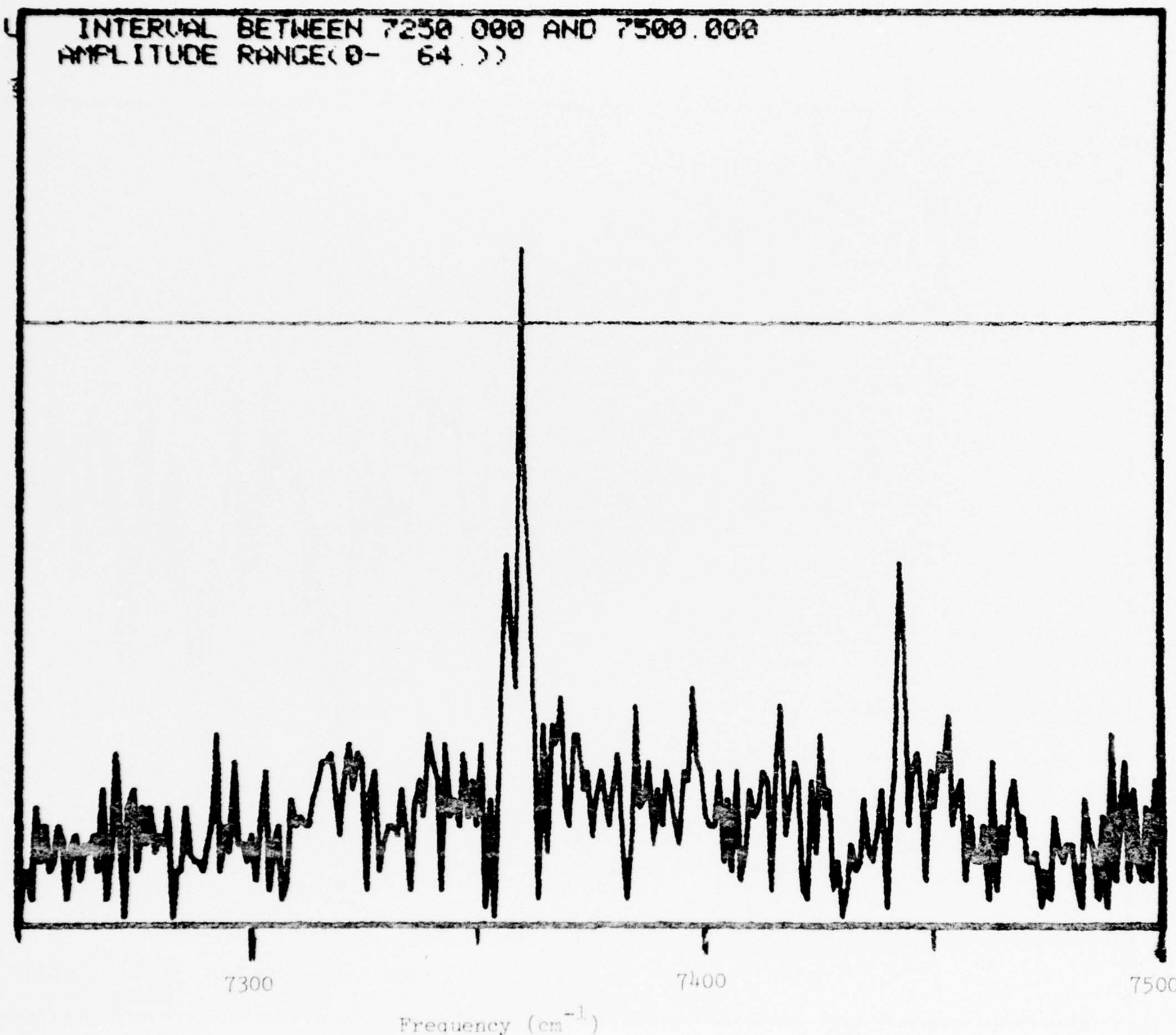
INTERVAL BETWEEN 7250.000 AND 7500.000
AMPLITUDE RANGE(0- 64.))
7300
7400
7500
Frequency (cm⁻¹)

Fig. 29

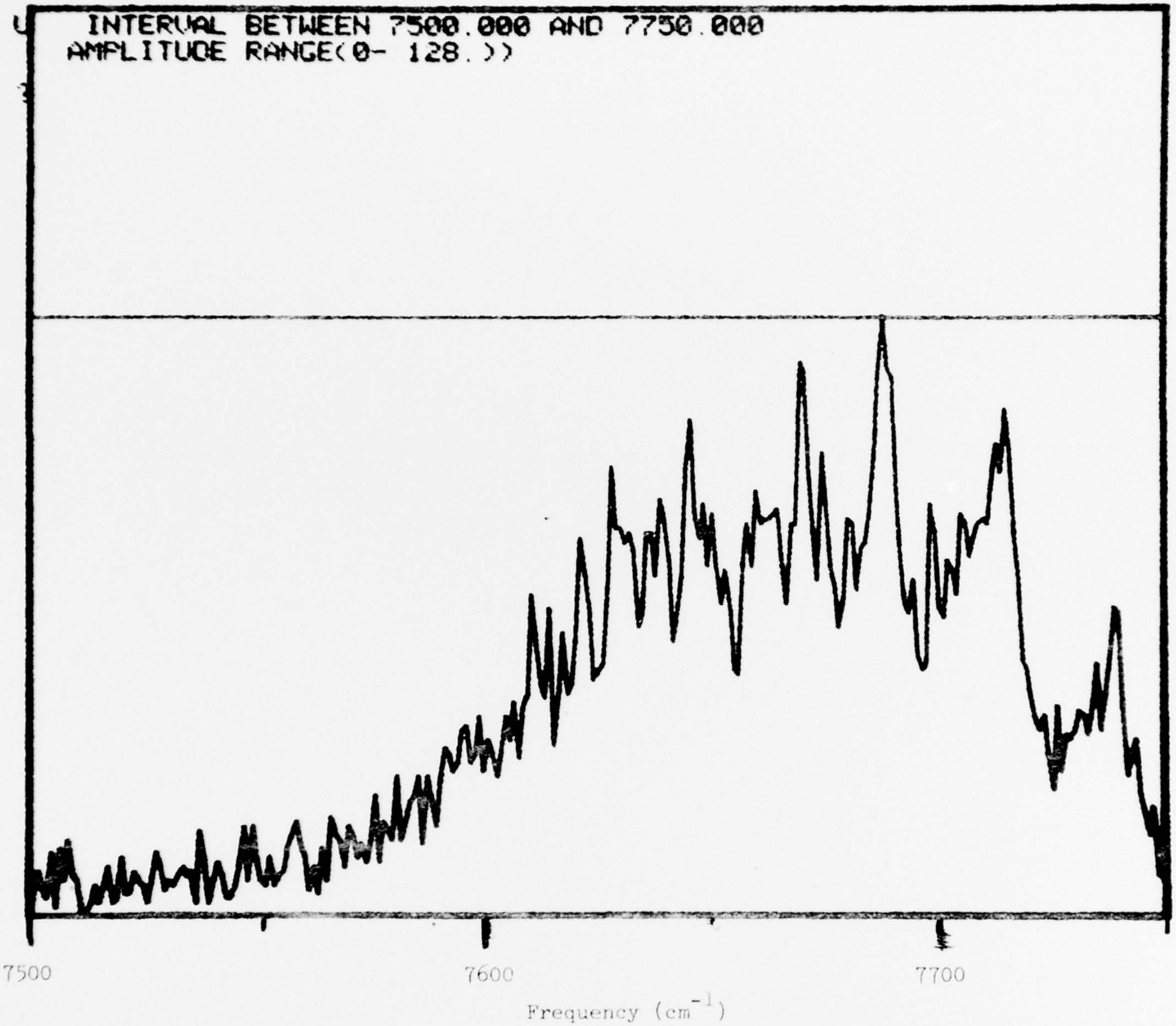
INTERVAL BETWEEN 7500.000 AND 7750.000
AMPLITUDE RANGE(0- 128.))
7500
7600
7700
Frequency (cm^{-1})

Fig. 30